ORNL/NRC/LTR-01/08

Contract Program or Project Title:	**Heavy-Section Steel Irradiation Program Metals and Ceramics Division**
Subject of this Document:	**Statistical Representation of Valid K_{Ic} Data for Irradiated RPV Steels**
Type of Document:	**Letter Report**
Authors:	**J. G. Merkle, M. A. Sokolov, R. K. Nanstad, and D. E. McCabe**
Date of Document:	**August 2002**
Responsible NRC Individual and NRC Office or Division:	**C. J. Fairbanks, 301-415-6719 Division of Engineering Technology Office of Nuclear Regulatory Research**

Prepared for the
U.S. Nuclear Regulatory Commission
Office of Nuclear Regulatory Research
Under Interagency Agreement DOE 1886-N695-3W

NRC JCN W6953

Prepared by the
OAK RIDGE NATIONAL LABORATORY
Oak Ridge, TN 37831-6151
Managed and Operated by
UT-Battelle, LLC
for the
U.S. DEPARTMENT OF ENERGY
Under Contract No. DE-AC05-00OR22725

ORNL/NRC/LTR-01/08

STATISTICAL REPRESENTATION OF VALID K_{Ic} DATA FOR IRRADIATED RPV STEELS

J. G. Merkle, M. A. Sokolov,
R. K. Nanstad, and D. E. McCabe

CONTENTS

ABSTRACT 1
INTRODUCTION 2
STATISTICAL APPROACHES 3
ANALYTICAL FORMULATION 5
APPLICATION TO THE ASME K_{Ic} DATABASE 8
COMPARISON OF MEASURED K_{Ic} VALUES WITH PREDICTIONS
BASED ON SMALL-SPECIMEN K_{Jc} DATA 16
General Considerations Regarding Size Effects 16
HSST Plate 02 19
ORNL Thermal Shock Experiments 20
DISCUSSION 26
CONCLUSIONS 28
ACKNOWLEDGMENTS 28
REFERENCES 28
APPENDIX A - EQUATIONS FOR CUMULATIVE PROBABILITY AND
PROBABILITY DENSITY FUNCTIONS FOR K_{Ic} A-1
APPENDIX B - SMALL-SPECIMEN FRACTURE-TOUGHNESS
CHARACTERIZATION DATA FOR ORNL THERMAL
SHOCK EXPERIMENTS B-1

STATISTICAL REPRESENTATION OF VALID K_{Ic} DATA FOR IRRADIATED RPV STEELS

J. G. Merkle, M. A. Sokolov,
R. K. Nanstad, and D. E. McCabe

ABSTRACT

The Heavy-Section Steel Irradiation Program at Oak Ridge National Laboratory (ORNL) includes various tasks associated with evaluation of the fracture toughness Master Curve, including its application to operating commercial reactor pressure vessels. A statistical representation of valid K_{Ic} data for the ferritic steels typically used in structures, piping, and pressure vessels has been derived by combining the principles of the elastic-plastic Master Curve of American Society for Testing and Materials (ASTM) E 1921 and the criterion for validity under elastic conditions contained in ASTM E 399. The equations derived are the direct result of the simultaneous solution of the equations for the Weibull size effect and the E 399 validity criterion. Both logic and experimental data support the approach presented. Specifically, extrapolation of the Weibull size effect to infinite specimen size produces an illogical result, and large-scale thermal shock data support the concept of K_{Ic}. The resulting equations for calculating tolerance bounds, cumulative probabilities, and probability density functions all exist in closed form. Furthermore, they preserve the present practice, justified by experiment, of treating the high-constraint fracture toughness of a steel as a material property independent of increases in component thickness and crack dimensions beyond those required for validity. By all evidence, the results obtained agree well with the American Society of Mechanical Engineers (ASME) K_{Ic} database, as well as the data from both large and small specimens for Heavy-Section Steel Technology (HSST) Plate 02 and the ORNL thermal shock experiments. These results therefore offer a promising approach for estimating values of K_{Ic} and their statistics based on small specimen fracture toughness data. This result presents a distinct advantage for irradiated nuclear reactor pressure vessels (RPVs), for which only small surveillance specimens are available for testing.

INTRODUCTION

Measuring the fracture toughness of the ferritic steels used for fabricating reactor pressure vessels (RPVs) requires dealing explicitly with the effects of temperature, specimen dimensions, yielding, and inherent scatter. Because of the relatively high fracture toughness values of most ferritic steels, testing specimens large enough to fracture in the linear elastic range is usually impractical. This is the reason for testing according to ASTM E 1921, which provides procedures for measuring the fracture toughness of ferritic steels with small specimens that yield before fracturing.[1] However, solving the experimental problem of measuring values of fracture toughness does not automatically solve the problem of how to apply the values obtained. Because cleavage fracture toughness decreases with increasing specimen size, at least until some limiting size is reached, and most pressure vessels remain nominally elastic in their plain cylindrical regions under their postulated design and accident loads, regulatory procedures for fracture prevention in pressure vessels are usually formulated in terms of the expected lower asymptotic value of fracture toughness defined by ASTM E 399 as K_{Ic}.[2] This creates a dilemma, because the fracture toughness values measured according to E 1921 are not K_{Ic} values, they are the larger K_{Jc} values either measured as or transformed to be descriptive of the fracture toughness of 1T specimens.[3,4] Furthermore, the known theoretically based statistical description of the scatter of K_{Jc} (1T) data and its companion empirical Master Curve (MC) are not applicable unchanged to representing the mean variation with temperature and the scatter of valid K_{Ic} data.[5] Because of this dilemma, multiple empiricisms are presently required to make even partial use of fracture toughness data obtained according to ASTM E 1921,[6] and this potentially could hamper the effective use of irradiated surveillance data.

Existing proposed procedures for making direct use of MC fracture toughness data in the safety assessment of RPVs involve either the use of a substitute value for RT_{NDT} based on an assumed relation between the substitute value and the characterizing temperature of the Master Curve, T_o,[6-8] or the use of a 5% lower tolerance bound (LTB) curve for 1T specimen data as a reference fracture toughness curve.[9] The latter proposal has two shortcomings. The first is that the proposed method does not include a complete statistical description, necessary for probabilistic fracture mechanics calculations, of the scatter of the fracture toughness values to be used for RPV analysis. The second shortcoming is that existing regulations are premised on the experimentally based concept of a lower asymptotic and size-independent value of fracture toughness defined as K_{Ic}.[2]

The latter concept of K_{Ic} has served well for over 30 years and it is not likely to be replaced for regulatory purposes unless overwhelming experimental evidence indicates its obsolescence. On the contrary, there are two sound reasons to retain the concept of K_{Ic} for RPV evaluations. The first is the observation that the Weibull size-effect equation, extrapolated to infinite specimen size, leads to a calculated fracture toughness value equal to the minimum value of 20 MPa$\sqrt{m}$ at any temperature, which is physically unrealistic.[3,10] This observation implies that there must be a specimen size beyond which the Weibull size-effect equation does not govern the fracture toughness.[5] The second reason is that existing experimental data do not support an unlimited extrapolation of the Weibull size effect equation. A small number of fracture toughness values obtained for A 533B steel with 10- and 11-in.-thick (254- and 279-mm) compact specimens consistently exceed the 95% upper tolerance bound (UTB) predictions when adjusted to 1T specimen size.[5,6] Also, the directly relevant large scale thermal shock tests performed on thick-walled hollow cylinders of A 508 chemistry forging steel by the HSST Program at ORNL demonstrated that the fracture toughness values for the first initiations of both short and long shallow cracks subjected to high, equibiaxial, thermal stresses populate the same scatter band defined by the original valid ASME K_{Ic} database.[11-13] More will be said about these data later. Consequently, it is reasonable to postulate that the fracture toughness of ferritic steel follows the Weibull size-effect equation only to a calculated specimen size that produces an elastically valid value of K_{Ic}, beyond which fracture toughness values become effectively independent of further increases in specimen size. Furthermore, prudence and satisfactory experience support the continued use of K_{Ic} values in fracture safety assessments. It is not necessary to explain this experimentally based approach theoretically. However, the use of the higher of two fracture toughness criteria can be viewed as requiring that two criteria both be satisfied for macroscopically unstable fracture to occur in the transition range, the first being a varying, size-dependent, toughness criterion for the formation of cleavage microcracks, and the second being a fixed but minimum-size related toughness criterion for the ductile separation of remaining ligaments between the microcracks.[14]

STATISTICAL APPROACHES

To date, a physically based and experimentally confirmed statistical description of fracture toughness in the transition range (the Weibull, weakest-link theory) has been developed to explain the performance of in-plane loaded, through-cracked laboratory specimens.[3,4,15] However, this theory has not yet been shown to unequivocally describe the performance of structures containing variously shaped surface and buried flaws. The

latter objective may never be fully achieved, but existing experimental data tend to support the hypothesis that loading and geometry play important roles, with equal biaxial stresses, especially in the presence of steep stress gradients, leading to high constraint and the dominance of K_{Ic}.[12] Thus, a statistical description of the scatter of elastically valid K_{Ic} values is an important component of a probabilistic fracture mechanics analysis method for critical structures such as RPVs.

Three attempts have been made to characterize the statistical behavior of valid, plane strain, K_{Ic} values. Sokolov[5] studied the relationship between the tolerance bounds of the 1T MC[1] and the ASME K_{Ic} database.[16,17] It was observed that the MC tolerance bounds fit the ASME database very well when the database was first adjusted to 1T specimen size. It was also observed that, because of the relatively low sensitivity to specimen size of the 5% and lower MC tolerance bounds, these lower tolerance bounds also agreed quite well with the lowest data in the as-measured (size-unadjusted) ASME K_{Ic} database. However, because the same degree of agreement between the MC tolerance bounds and the size-unadjusted, valid, K_{Ic} database does not extend to higher cumulative probability levels, the statistics of the Master Curve do not provide a comprehensively accurate description of the statistics of valid K_{Ic} data.

Wallin[18] also examined the ASME database with the intent of estimating the effective cumulative probability-of-failure levels corresponding to the ASME K_{Ic} curve, and to the 5% and lower MC tolerance bound curves. The approach was to rank, in order of increasing magnitude, the temperature margins between individual toughness values in the ASME K_{Ic} database and the curves of interest, and then fit the results for each curve to a cumulative probability distribution. The results showed that the cumulative probabilities of zero temperature margins for the ASME K_{Ic} curve and the 5% lower MC tolerance bound curve were both about 2%.[18] Thus, the ASME K_{Ic} curve and the 5% lower MC tolerance bound curve have an approximate statistical equivalence. The nonequality of the estimated failure probability for the 5% lower MC tolerance bound curve and the percentile associated with that curve was not explained. Also, no attempt was made in Ref. 18 to develop a statistical description of the variability of valid K_{Ic} data.

In response to the need for a quantitative description of the variability of valid K_{Ic} data in terms of mathematical statistics for use in pressurized thermal shock (PTS) analyses for RPVs, Bowman and Williams,[19] and Williams et al.,[20] developed an empirical mathematical model based on the equation of the three-parameter Weibull distribution. In this model, all three parameters were taken as empirical functions of $(T - RT_{NDT})$ by

means of equations of the same form as the ASME K_{Ic} curve. A particularly important feature of this model is that the empirical value of the Weibull exponent resulting from choosing RT_{NDT} as the normalizing temperature is significantly less than 4. At values of ($T - RT_{NDT}$) equal to -100, 0, and 60°F, the values of the Weibull exponent are 2.16, 2.53, and 3.15, respectively. Because scatter, and therefore uncertainty, increase as the Weibull exponent decreases, this model inherently predicts a greater degree of uncertainty than is associated with the Master Curve.

Recognizing the degree of uncertainty associated with RT_{NDT} as well as its generally conservative bias, Williams et al. recently reformulated the Bowman-Williams model by means of a change of variable and some additional data.[20] The reference temperature in the new toughness model has been changed from RT_{NDT} to RT_{LB}, the latter being a new indexing temperature that positions the ORNL HSST modified ASME K_{Ic} curve[17] so that it actually lower bounds the complete individual sets of data in the ASME K_{Ic} database. Several variants of the new model have been developed, with different combinations of fixed and empirically evaluated parameters. The variant selected for recommended use in PTS analyses[21] has a fixed Weibull slope of 4, with the other two parameters being evaluated empirically, as described. Choosing a Weibull slope of 4 might appear to reduce the implied uncertainty associated with the new model to a degree consistent with the MC approach, but because there is no practical way to experimentally measure RT_{LB} directly for a particular material in a vessel, this is actually not the case. It is necessary to estimate RT_{LB} through its probabilistic relation with RT_{NDT} so that the original uncertainty associated with RT_{NDT} has been partitioned between two functions; the first function being the probabilistic relation between RT_{NDT} and RT_{LB}, and the second function being the correlation between K_{Ic} and ($T - RT_{LB}$).

ANALYTICAL FORMULATION

The basic premise of the approach to be explained here is that the two hypotheses, one of a Weibull size effect on fracture toughness caused by the weakest-link behavior of elements near the crack front, and the other of a size-independent value of fracture toughness beyond a certain size, are both true, at least to a degree of approximation sufficient for engineering application. The consequences of this premise, illustrated in Fig. 1, have already been examined analytically by McCabe and Merkle,[22] in terms of

ORNL 2001-04106/rra

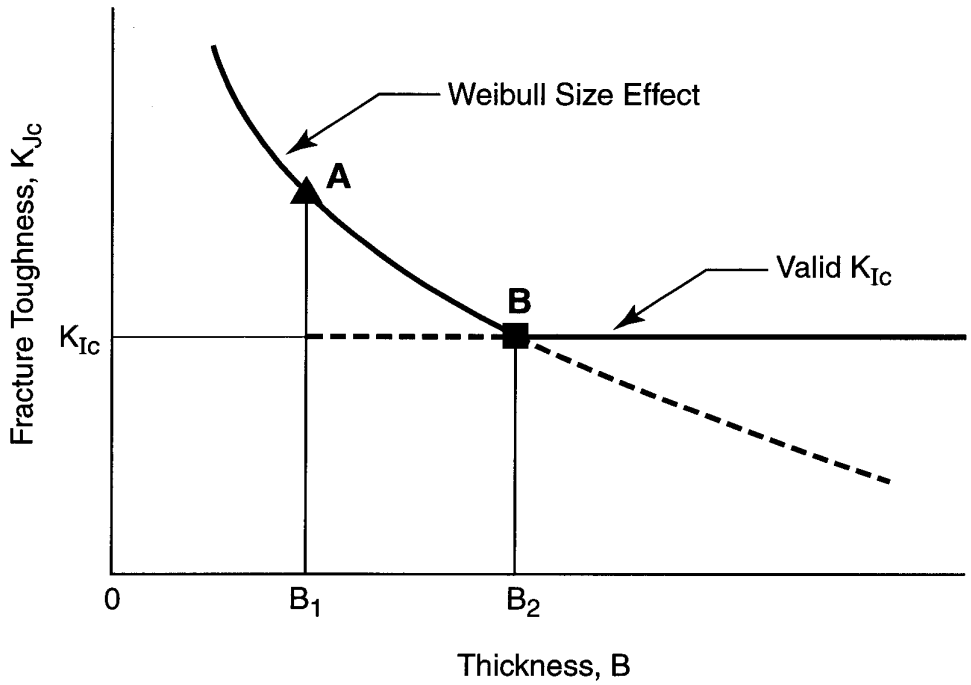

Figure 1. Schematic representation of the curves for the Weibull size effect, and the linear elastic K_{Ic} validity criterion of ASTM E 399.

locating the intersection of the Weibull size-effect curve for relatively small specimen sizes with a horizontal line of constant fracture toughness for specimen sizes equal to and greater than the smallest specimen capable of producing a valid value of fracture toughness. The mathematical results presented in Ref. 22 were originally suggested for use when specimens are too few in number to apply a statistical approach. However, these mathematical results are by no means limited to that one situation and, in fact, they provide a gateway to estimating K_{Ic} values and their statistics from measurable values of K_{Jc} obtained from small specimens, and the statistics of the Master Curve.

As explained in Ref. 22, the simultaneous solution of the Weibull size-effect equation,

$$K_{Jc(2)} = (K_{Jc(1)} - K_{\min}) \left(\frac{B_1}{B_2} \right)^{1/4} + K_{\min} , \tag{1}$$

in which the subscripts 1 and 2 represent the specimen size tested, and a second size, large enough to be valid, respectively, with a generalization of the ASTM E 399 validity criterion of linear elastic fracture mechanics (LEFM),

$$B_2 = \alpha_0 \left(\frac{K_{Ic}}{\sigma_Y} \right)^2 , \tag{2}$$

leads to the cubic equation

$$\left(\frac{K_{Ic}}{K_{\min}} \right)^{3/2} - \left(\frac{K_{Ic}}{K_{\min}} \right)^{1/2} - 2G = 0 , \tag{3}$$

in which

$$2G = \left(\frac{K_{Jc(1)}}{K_{\min}} - 1 \right) \left(\frac{\sqrt{B_1/\alpha_0}}{K_{\min}/\sigma_Y} \right)^{1/2} . \tag{4}$$

Equation (3), which results from setting $K_{Jc(2)} = K_{Ic}$ and substituting Eq. (2) into Eq. (1), locates point B in Fig. 1, the coordinates of which are B_2, the limiting specimen size beyond which Eq. (1) is no longer operative, and K_{Ic}, the valid linear elastic fracture

mechanics (LEFM) value of fracture toughness. The analytical solution of Eq. (3) is accomplished by means of three substitutions followed by a direct calculation. Let*

$$M_1 = G + \sqrt{G^2 - (1/3)^3} \ , \tag{5}$$

$$M_2 = G - \sqrt{G^2 - (1/3)^3} \ , \tag{6}$$

and

$$y = M_1^{1/3} + M_2^{1/3} \ . \tag{7}$$

Then

$$K_{Ic} = y^2 K_{\min} \ . \tag{8}$$

APPLICATION TO THE ASME K_{Ic} DATABASE

The initial means for observing the potential accuracy with which the proposed approach can provide a statistical description of valid K_{Ic} data is to construct tolerance-bound plots for the ASME database, plotted both in terms of the data adjusted to 1T specimen size, and the unadjusted, as-measured data. The former plot, shown in Fig. 2, has already been presented by Sokolov.[5] Additionally, Sokolov[5] also presented Fig. 3, which demonstrates the approximately accurate relationship between the 5, 3, and 1% MC lower tolerance bound curves and the unadjusted ASME database. The accuracy displayed in Fig. 3 is due to the relatively low size sensitivity of the lower MC tolerance bound curves.

The comparisons illustrated in Figs. 2 and 3 are encouraging, but they are still subject to the limitation of being based on a single set of elastically valid experimental data, and the

*Note that the algebraic signs under the radicals in Eqs. (5) and (6) were inadvertently omitted in Ref. 22.

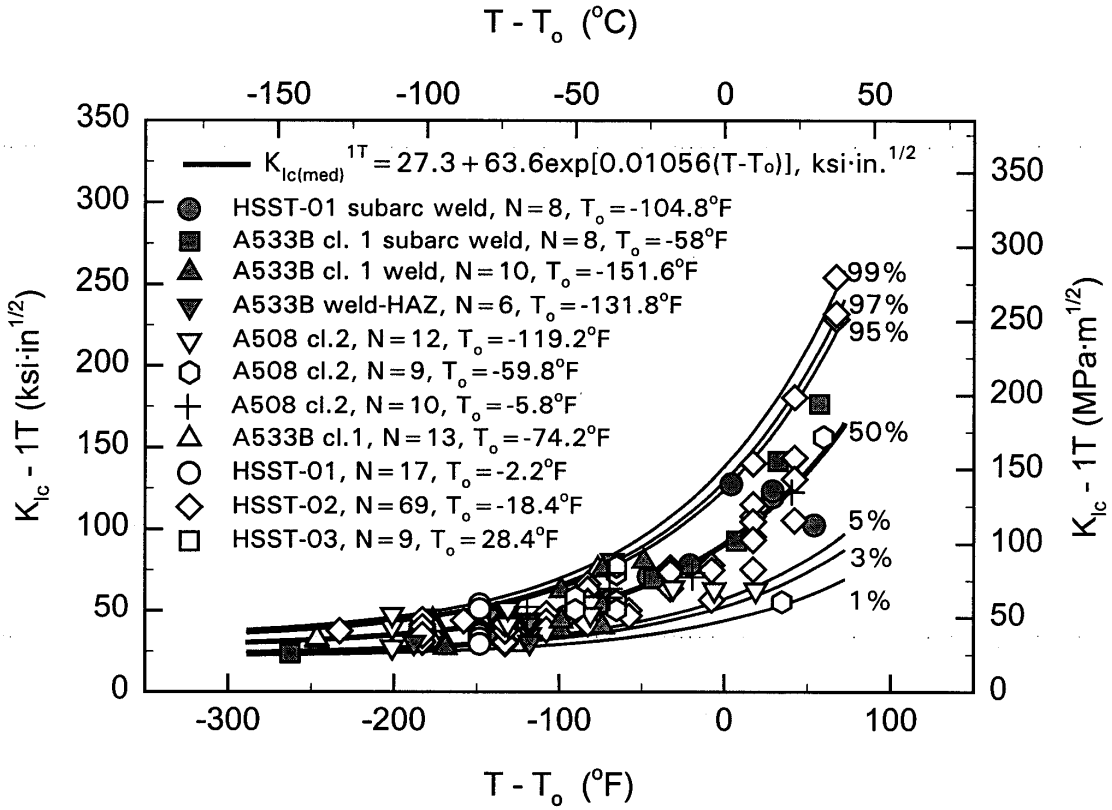

Figure 2. Fig. 2. The ASME K_{Ic} data statistically adjusted to 1T specimen size equivalence and described by the Master Curve and its corresponding upper and lower tolerance bounds (from Ref. 5).

accompanying assumption that the size effects are purely statistical in nature and perfectly described by Eq. (1). This means that any potential additional effects of triaxial constraint associated with specimen size are not revealed. To observe such additional size effects requires two independent sets of experimental data, one for small specimens and the other for specimens large enough to produce essentially elastically valid data. Two such comparisons will be presented later in this report.

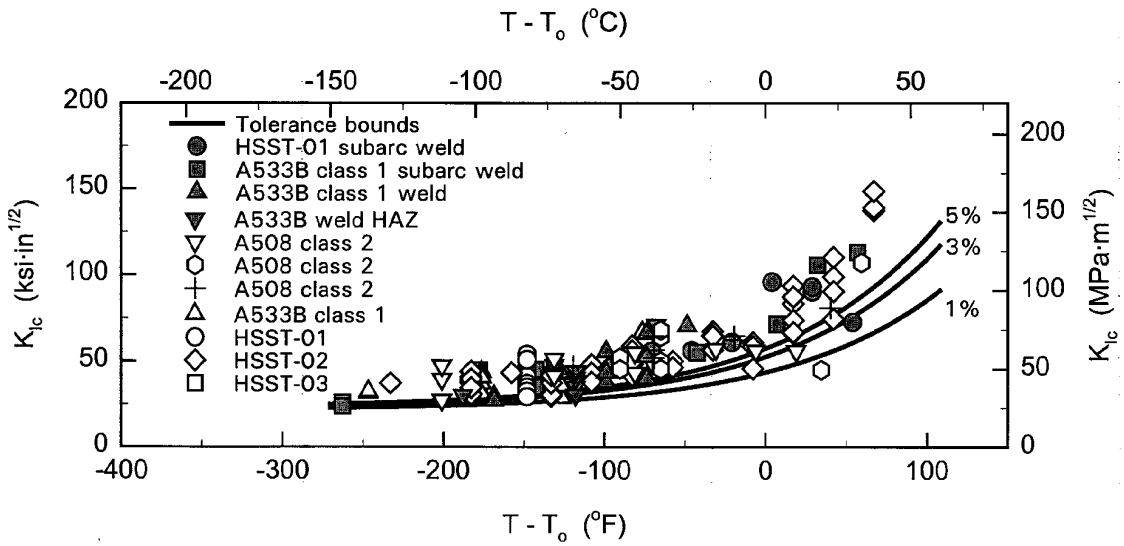

Figure 3. The ASME K_{Ic} database versus temperature, normalized by T_o, plus the 5, 3, and 1% 1T Master Curve tolerance bound curves (from Ref. 5).

The equations for calculating a tolerance bound curve for K_{Ic} data based on the statistics of the Master Curve all exist in closed form. The strategy is simply to convert the value of $K_{Jc(1T)}$ obtained from the equation of the corresponding 1T MC tolerance bound curve to its corresponding value of K_{Ic}, using Eqs. (4) through (8). Solving the Weibull cumulative probability equation,

$$P_f = 1 - e^{-\left(\frac{K_{Jc} - K_{\min}}{K_o - K_{\min}}\right)^4} \tag{9}$$

for K_{Jc} gives

$$K_{Jc} = K_{\min} + (K_0 - K_{\min})\left[\ln\left(\frac{1}{1-P_f}\right)\right]^{1/4} . \tag{10}$$

Also, from Eq. (10), for $P_f = ½$ and $K_{Jc} = K_{Jc(1T,med)}$,

$$(K_0 - K_{\min}) = \frac{K_{Jc(1T,med)} - K_{\min}}{(ln2)^{1/4}} , \tag{11}$$

where the value of K_0 is the scale parameter associated with data adjusted to 1T specimen size.

Using the equation of the Master Curve, Eq. (11) becomes

$$(K_0 - K_{\min}) = \frac{30 - K_{\min} + 70e^{0.019(T - To)}}{(ln2)^{1/4}} , \tag{12}$$

so that substituting Eq. (12), with K_{min} = 20 MPa$\sqrt{m}$, into Eq. (10) gives

$$K_{Jc} = 20 + \left[\frac{\ln\left(\frac{1}{1-P_f}\right)}{ln2}\right]^{1/4} [10 + 70e^{0.019(T - To)}] , \tag{13}$$

which is the equation of a specific MC tolerance bound curve. Equations (4) through (8), applied to the results of Eq. (13), with B_1 = 0.0254 m, then produce the values of K_{Ic} for plotting the corresponding tolerance bound curve for K_{Ic}. For purposes of comparison, it is also useful to plot the ASME lower bound K_{Ic} curve, repositioned[6-8] according to ASME Code Cases N-629 and N631.[23,24] The equation of the ASME K_{Ic} curve is[16,17]

$$K_{Ic} = 36.5 + 22.8e^{0.036(T - RT_{NDT})}, \tag{14}$$

in which K_{Ic} is in MPa$\sqrt{m}$ and (T - RT_{NDT}) is in °C. The adaptation of Eq. (14) for use with data obtained according to the Master Curve is by means of the replacement of RT_{NDT} by a temperature called RT_{To}, and the assumed relationship[6-8,23,24]

$$RT_{To} = T_o + 19.4°C \ . \tag{15}$$

Substituting Eq. (15) into Eq. (14) then gives

$$K_{Ic} = 36.5 + 11.3e^{0.036(T - T_o)}. \tag{16}$$

Figure 4 shows the relationship between the calculated 98, 50 (median), and 2% tolerance bound curves for K_{Ic}, based on $\alpha_o = 2.5$ and $\sigma_Y = 482.6$ MPa (70 ksi), plus the repositioned ASME K_{Ic} curve and the ASME database, with K_{Ic} values plotted as measured. The agreement is quite good, supporting the premise that a statistical description of valid K_{Ic} data is obtainable by the proposed approach.,[25,26]

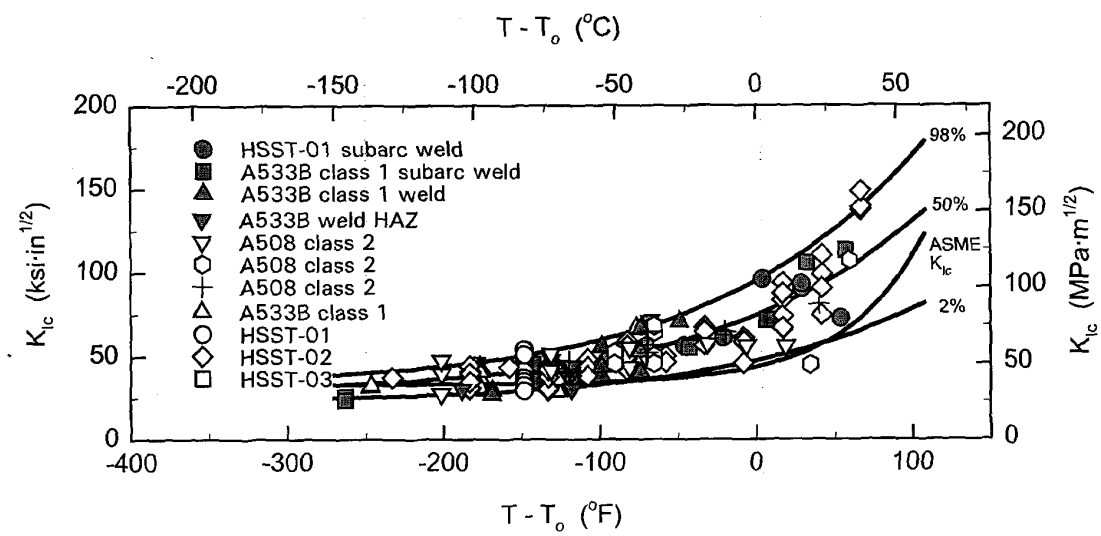

Figure 4. The ASME K_{Ic} database versus (T - T_0), plus calculated 98, 50 (median), and 2% tolerance bound curves for K_{Ic}, for $\sigma_Y = 482.6$ MPa (70 ksi) and $\alpha_0 = 2.5$.

The calculations made for the purpose of plotting the tolerance bound curves shown in Fig. 4 reveal one aspect of the analysis that requires refinement, as illustrated in Fig. 5. In applying the hypothesis that K_{Ic} occurs at the intersection of the Weibull size-effect

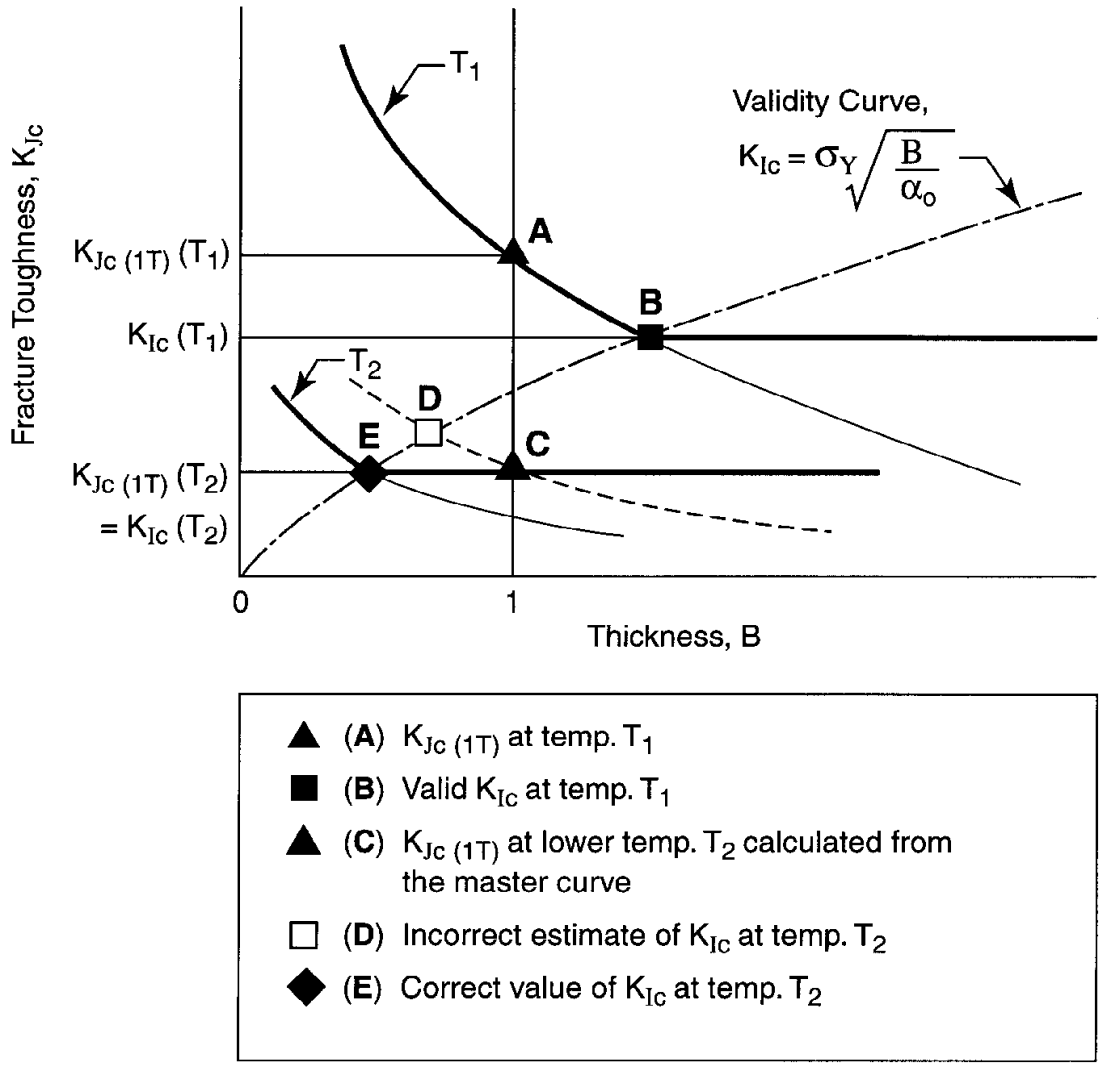

Figure 5. Schematic curves illustrating the logic for determining K_{Ic} when data valid by ASTM E 399 can be obtained with specimens of 1T size or smaller.

curve with the ASTM E399 validity curve, it is necessary to avoid an unconservative estimate of K_{Ic} that can occur at low temperatures or low tolerance bound levels. Suppose that, for a given tolerance bound, the variation of toughness with specimen size at test temperature T_1, is as shown in Fig. 5, with the toughness value obtainable from a 1T specimen being identified by point A, and the K_{Ic} value being identified by point B. Also, suppose that at a lower temperature, T_2, and for the same tolerance bound level, the

calculated value of $K_{Jc(1T)}$ from the equation of the MC tolerance bound curve is identified by point C. Assuming that toughness immediately increases with decreasing specimen size beginning at point C, as indicated by the broken curve, and that K_{Ic} is identified by point D, would be unconservative, because toughness should remain constant with decreasing specimen size between point C and the size of K_{Ic} validity. Therefore, for values of $K_{Jc(1T)}$ that are valid K_{Ic}, toughness should be considered to remain constant between points C and E, and then it should be considered to increase with further decreases in specimen size. In this regime, the tolerance bound curves are calculated by using Eq. (13) without using Eqs. (4) through (8). For a given tolerance bound level, the value of $K_{Jc(1T)}$ at and below which such values are valid can be obtained by solving Eq. (2) for K_{Ic}, giving

$$K_{Ic} = \sigma_Y \sqrt{\frac{B_2}{\alpha_o}} , \tag{17}$$

in which B_2 is the thickness of a 1T specimen. The value of $(T - T_o)$ at and below which values of $K_{Jc(1T)}$ are valid is found by substituting the value of K_{Ic} obtained from Eq. (17) for $K_{Jc(1T)}$ in Eq. (13), and solving for $(T - T_o)$, giving

$$(T - T_o) = \frac{1}{0.019} \ln \left\{ \frac{\dfrac{(K_{Ic} - K_{\min})}{\left[\dfrac{\ln\left(\dfrac{1}{1 - P_f}\right)}{ln2} \right]^{1/4}} - 10}{70} \right\} . \tag{18}$$

The adjustments resulting from this refinement are usually small, typically being of the order of 2 MPa$\sqrt{\mathrm{m}}$ or less.

For probabilistic calculations, it is necessary to have the equations of the cumulative probability distribution for K_{Ic}, and its first derivative, the probability density function (pdf), which is also called the frequency distribution, of K_{Ic}. The derivation of these equations is given in Appendix A.

A comparison of the tolerance bound curves associated with the 1T MC and valid K_{Ic} data is shown in Fig. 6. As implied previously in Ref. 5, the MC and K_{Ic} lower 2% tolerance bound curves are not much different. However, the higher tolerance bound curves, including the median curves, are significantly different in the mid and upper transition ranges because the 1T MC is not a curve of full constraint toughness. Figure 6 illustrates the toughness adjustments necessary for estimating K_{Ic} from small-specimen data, as well as demonstrates the feasibility of making such estimates by the method described here.

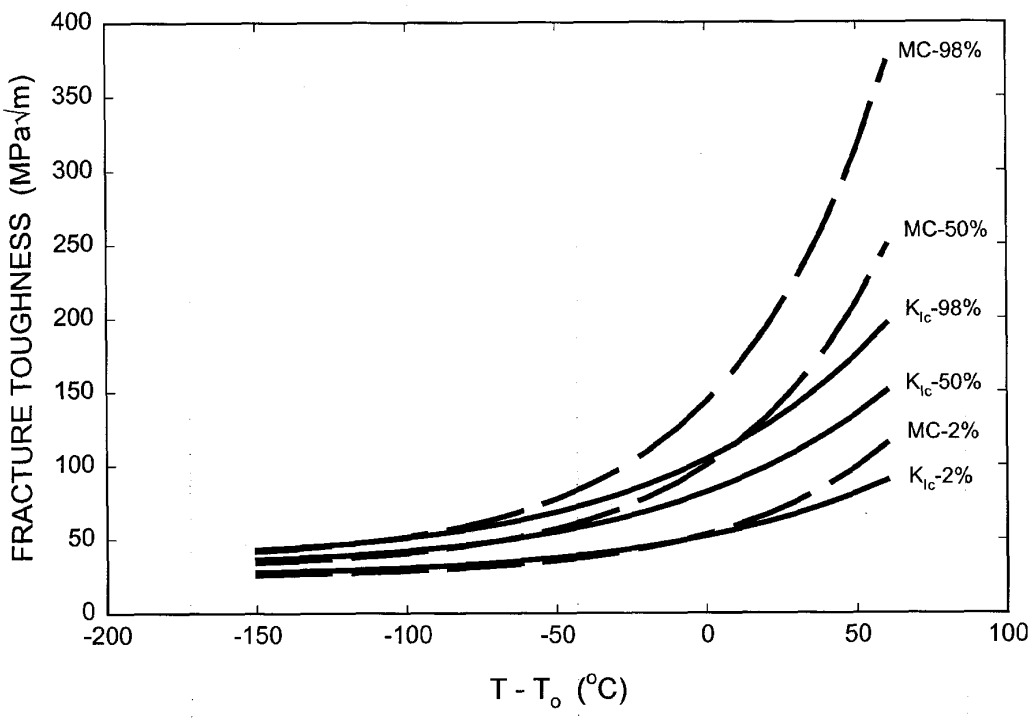

Figure 6. Comparison of tolerance bound curves associated with the 1T Master Curve and with valid K_{Ic} data, using σ_Y = 482.6 MPa (70 ksi) and α_0 = 2.5.

COMPARISON OF MEASURED K_{Ic} VALUES WITH PREDICTIONS BASED ON SMALL-SPECIMEN K_{Jc} DATA

General Considerations Regarding Size Effects

The foregoing discussion has demonstrated the viability of calculating the tolerance bounds for K_{Ic} data, based on combining concepts from ASTM standards E 399 and E 1921, when only valid K_{Ic} data are available and all size effects are assumed to be statistical in nature. However, it needs to be recognized that the most common problem in application involves the availability of only small-specimen K_{Jc} data, with the need to estimate the statistics for the corresponding high-constraint values of K_{Ic}. In this case, it can be hypothesized that all size effects may not be statistical in origin, but rather might be due to some unknown combination of statistical effects and triaxial constraint effects. Furthermore, it is possible that separating the size effects due to these two causes may be obfuscated by a similarity in the separately predicted trends for the two different causes. Considering this possibility, it was decided to make a preliminary comparison between the size effects predicted by the Weibull theory and those predicted by Irwin's empirical constraint-related β_{Ic} equation.[27-29] This comparison was considered potentially useful because the Irwin β_{Ic} adjustment had already provided a good reconciliation between the calculated values of K_{Ic} from the ORNL thermal shock tests and the available small-specimen fracture toughness data for the test cylinder materials.[27] The intent of the present comparison was to explore the known similarity in the predictions of the two methods.[28] by searching for a trial value of α_o that might empirically equate the two predictions, and thus implicity incorporate size effects due both to constraint and to weakest-link statistical behavior in the coupled Weibull E 399 calculations. Subsequent calculations by the method being proposed, comparing estimates of K_{Ic} based on small-specimen data with values measured directly with large specimens, would then be used to refine the choice of α_o, if necessary. In the process of performing these calculations it became apparent that, since the quantities α_o and σ_Y enter the calculations in only one combination, $\sigma_Y / \sqrt{\alpha_o}$, a parameter definable as a reference stress and given by

$$\sigma_R = \frac{\sigma_Y}{\sqrt{\alpha_o}} , \tag{19}$$

can be a useful and perhaps a physically more meaningful parameter than its two factors considered separately. Furthermore, one example, to be presented, indicated that σ_R may have a common, and temperature-independent, value for a general class of materials.

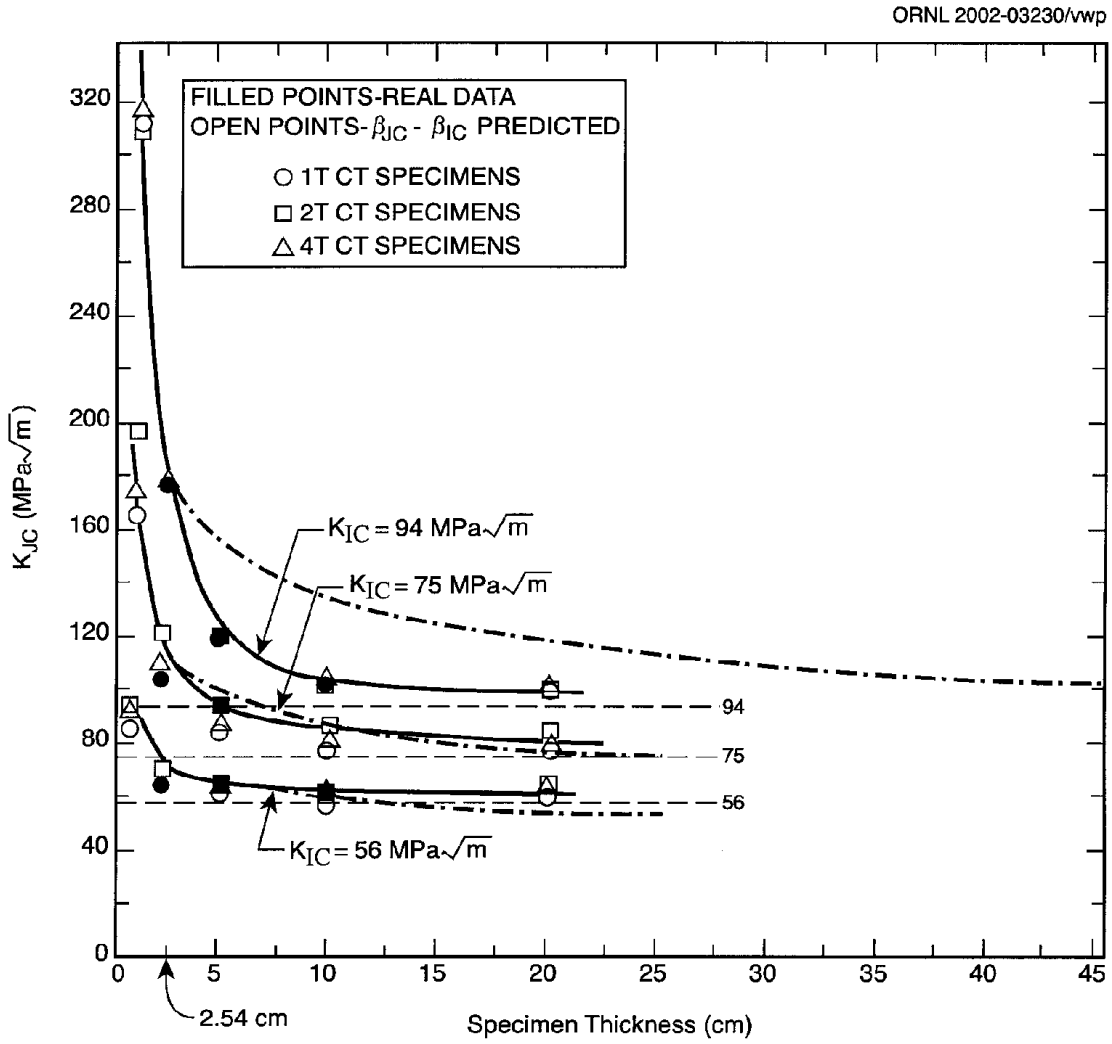

Figure 7. Comparison of size effect data with curves based on the Irwin β_{Ic} and Weibull equations for HSST Plate 13A.

A well-posed example for comparing Weibull and β_{Ic} predictions is illustrated in Fig. 7, which is an adaptation of Fig. 9 appearing in Ref. 29. The experimental data represented by the filled points in Fig. 7 are selected values for the plate of A533 grade B class 1 steel designated as HSST Plate 13A, for which the value of σ_Y was taken as 503 MPa (73 ksi). The open points in Fig. 7 are values calculated from Irwin's β_{Ic} equation,[28]

$$\beta_{Jc} = \beta_{Ic} + 1.4\,\beta_{Ic}^{\,3} \quad , \tag{20}$$

where

$$\beta_{Ic} = \frac{\left(\dfrac{K_{Ic}}{\sigma_Y}\right)^2}{B} \, , \tag{21}$$

and β_{Jc} is obtained by replacing K_{Ic} in Eq. (21) with K_{Jc}. The solid curves in Fig. 7 are drawn according to Eq. (20). Selecting three hypothetical values of $K_{Jc(1T)}$ close to the plotted points and the β_{Ic} curves at B = 2.54 cm in Fig. 7, the dash-dot Weibull size-effect curves were plotted from these points for comparison with the β_{Ic} curves. The selected values of $K_{Jc(1T)}$ and the values of K_{Ic} corresponding to the β_{Ic} curves are given in Table 1.

Table 1. Parameters leading to identical estimates of K_{Ic} by the Weibull and the Irwin β_{Ic} size effect equations

K_{Jc} (MPa$\sqrt{m}$)	K_{Ic} (MPa$\sqrt{m}$)	α_o
177	94	14.75
110	75	8.20
70	56	7.63

Inserting both these values into a rearrangement of Eqs. (3) and (4) produces the values of α_o shown in Table 1 that give identical estimates of K_{Ic} from both the Weibull and the β_{Ic} size-effect equations. For the three cases considered, the average calculated value of α_o is quite close to 10. Considering the approximations inherent in the foregoing calculations, this value was therefore selected for initial use in the example calculations to be performed for the two available sets of data comprising both small and large specimen toughness values for the same materials. Returning to Fig. 7, it can be seen that, for the two lower sets of data and their associated curves, the Weibull and the β_{Ic} curves are quite close to each other. However, for the upper set of data, the Weibull

curve undergoes a considerably more gradual downward transition than does the experimental data, which are followed quite closely by the associated β_{Ic} curve. This implies that constraint effects are combined with statistical size effects for relatively high values of $K_{Jc(1T)}$, for specimen sizes bordering on 1T, with the result that the intercept of the Weibull size-effect curve with the estimated K_{Ic} line occurs at a specimen thickness considerably beyond that expected for the actual experimental data. However, since the calculated size corresponding to K_{Ic} is only a means to an end, this is not necessarily an impediment as long as the estimate of K_{Ic} itself is accurate.

HSST Plate 02

Following the demonstration, by means of large-scale dynamic tear tests at the Naval Research Laboratory, that the fracture toughness of pressure vessel steel undergoes a steep transition with temperature, even in thick sections, [30] large-scale measurements of valid static K_{Ic} values for HSST Plate 02, covering its brittle-to-ductile transition temperature range, were made by the Westinghouse Research Laboratory.[31] The resulting median curve of K_{Ic} versus temperature for HSST Plate 02, shown in Fig. 8, became known as the Million Dollar Curve. These data also served as the principal basis for drawing the ASME lower-bound K_{Ic} curve.[16] More recently, with the advent of the technology underlying the Master Curve approach[3,4] and its codification in terms of ASTM Standard E 1921,[1] keen interest has developed in using specimens as small as precracked Charpy (PCCV) specimens for determining the fracture toughness of structural and pressure vessel steels. Sokolov, Wallin, and McCabe[32] made measurements of K_{Jc} for HSST Plate 02 with PCCV specimens, obtaining valid data sets at -50 and -30°C. The values of K_{Jc} obtained provide a good opportunity to evaluate the proposed method of estimating K_{Ic}, by constructing a comparison between K_{Ic} values estimated based on small-specimen data and directly measured valid values obtained with sufficiently large specimens. In this comparison, all size effects that exist will be revealed. Table 2 lists the highest and the lowest values of K_{Jc} measured at -50 and -30°C with PCCV specimens, along with the values of σ_Y scaled from Fig. 8 at these two temperatures, plus the resulting values of K_{Ic} estimated by Eqs. (4) through (8), using $\alpha_o = 10$. The ranges of the estimated values of K_{Ic} based on PCCV data, as given in Table 2, are plotted in Fig. 8. Both ranges bracket the Million Dollar Curve (the median curve of directly measured K_{Ic} values) quite well, indicating success in predicting K_{Ic} values based on small-specimen data.

Table 2. Estimated ranges of K_{Ic} for HSST Plate 02, based on K_{Jc} data from PCCV specimens given in Ref. 27, and $\alpha_o = 10$

T (°C)	K_{Jc} (MPa$\sqrt{m}$)	σ_Y (MPa)	Estimated K_{Ic} (MPa$\sqrt{m}$)
-50	79.23	524	53.09
	101.67	524	62.17
-30	96.20	510	59.63
	131.35[a]	510	72.51

[a] $K_{Jc(limit)}$.

ORNL Thermal Shock Experiments

From 1975 to 1985, the HSST Program at ORNL conducted a series of carefully designed and controlled thermal shock experiments (TSEs) using thick-walled cylinders of specially heat-treated A508 class 2 chemistry steel containing inner-surface cracks, prepared and sharpened by electron-beam welding and hydrogen charging and thermally shocked with liquid nitrogen.[11] Prolongations of the test cylinders provided a source of pretest material characterization specimens, as well as did the cylinders themselves for post-test examination. The object of the experiments was to determine if linear elastic fracture mechanics (LEFM) could be used to characterize the fracture behavior of pressure vessel steels under thermal shock loading. The test materials were characterized both in terms of RT_{NDT} and fracture toughness obtained from relatively small specimens. The validation of LEFM for thermal shock loading was by means of showing that the K_{Ic} values calculated for the TSEs fell substantially within the same scatter band characterizing the ASME-EPRI K_{Ic} database, plotted versus ($T - RT_{NDT}$).[11] This result also demonstrated, as a corollary, that although the initial cracks in the TSE cylinders were shallow, this fact had no apparent effect on the calculated fracture toughness values, with respect to K_{Ic}, for thermal shock loading. The fracture toughness data obtained from the relatively small characterization specimens of the TSE materials were used qualitatively for test temperature selection and test evaluation, but not quantitatively for validating LEFM, because of an incomplete understanding at the time of the size effects involved.

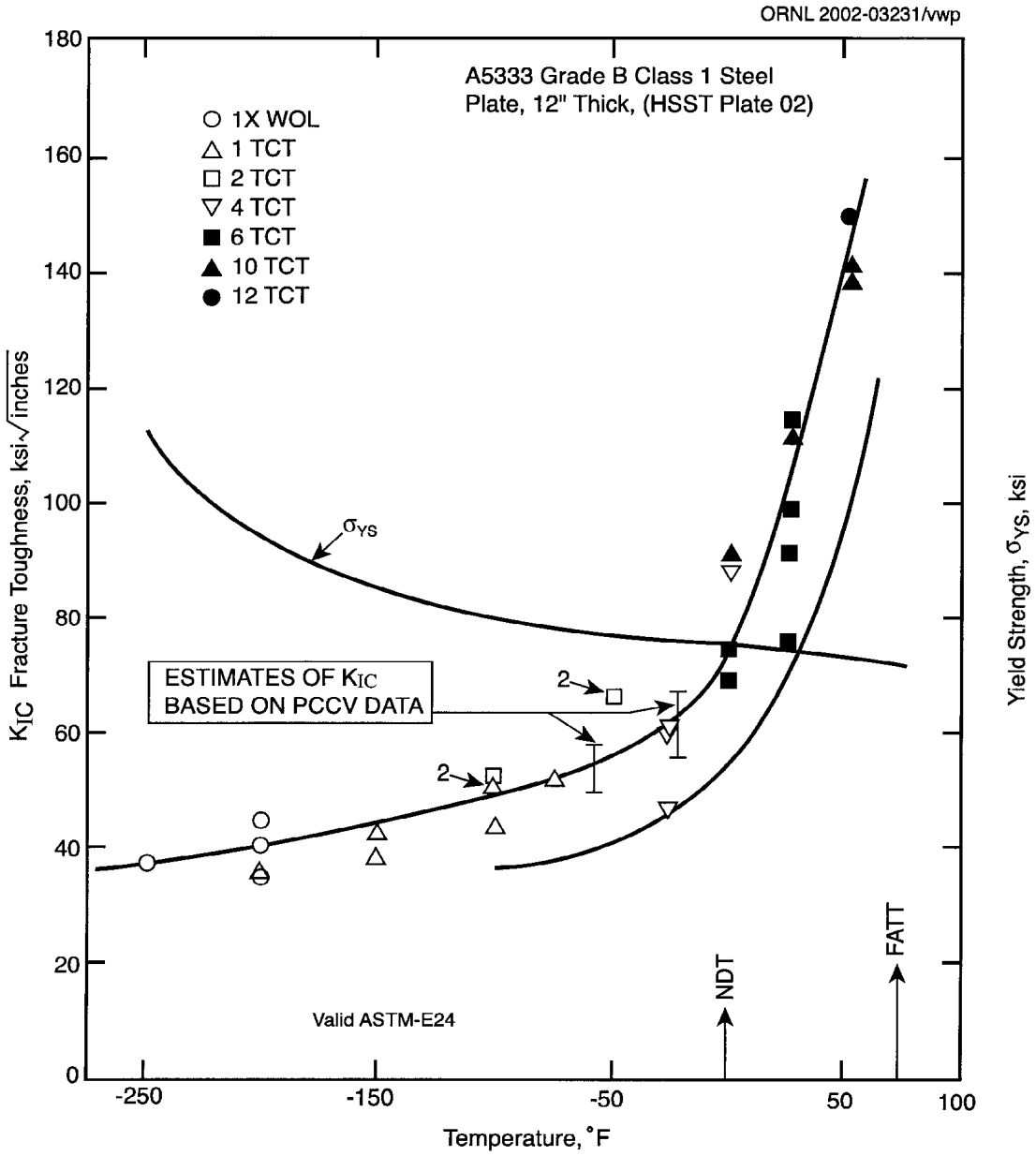

Figure 8. Comparison of predicted ranges of K_{Ic} based on PCCV data with directly measured LEFM valid data for HSST Plate 02 at -50 and -30°C (-58 and -22°F).

Following the thermal shock tests, efforts were made to better understand the size effects and data scatter characteristic of small-specimen fracture toughness testing. Irwin's β_{Ic} adjustment, based on the concept of through-thickness constraint effects, had proven helpful in understanding the behavior of inside nozzle corner cracks in pressure vessels subjected to internal pressure loading.[33] This concept was therefore applied to an

attempted reconciliation of the small specimen fracture toughness data for the TSE materials with the directly measured K_{Ic} values. Good success was achieved, except at the highest specimen test temperatures, at which prior stable crack growth and/or fracture after maximum load may have led to some underpredictions of K_{Ic}.[27] At the same time, efforts were under way to understand the statistical variability, as well as the size effects, characterizing fracture toughness data in the transition range for structural and pressure vessel steels. Eventually these efforts led to the development of the Master Curve approach[3,4] and to its standardization in the form of ASTM Standard E 1921.[1] During this process, Wallin[34] reanalyzed the ORNL TSE data and its accompanying small-specimen fracture toughness characterization data, concluding that all the data were subject to Weibull size effects, and confirming the null effect of initial shallow crack depths on fracture toughness for the TSEs. The finding concerning size effects led Wallin to conclude that the statistical size effect can exist even for valid K_{Ic} data,[34] a position reiterated[35] by stating that, "The classical interpretation of K_{Ic} as being a lower bound, specimen size insensitive, fracture toughness value corresponding to a plane-strain stress state is wrong." Wallin's conclusions about crack length size effects were dependent upon test-specific guesses concerning the lower limit of the upper-shelf temperature range, and the effective crack length for finite-length surface cracks. For these reasons, and because the Weibull size effect becomes quite weak at long crack lengths, Wallin's conclusions are not considered complete proof here that K_{Ic} does not exist. Furthermore, the previously achieved good reconciliation between small and large specimen test data for the TSEs, by means of the Irwin β_{Ic} adjustment, combined with the achievement of approximate consistency between the Irwin β_{Ic} adjustment and the currently proposed Weibull E 399 adjustment, with $\alpha_o \sim 10$, plus the accurate estimates of K_{Ic} based on PCCV data for HSST Plate 02 by the currently proposed method, are collectively considered grounds for postulating that small and large specimen TSE data can also be reconciled in terms of K_{Ic} by the currently proposed method.

The data to be analyzed here are for four thermal shock tests performed at ORNL on 991-mm OD (39-in.) cylinders of A508 class 2 steel, specially heat treated to control yield stress and toughness, and for which the experimental data are considered quite accurate in all important respects. A summary of test conditions is given in Table 3, compiled from the information tabulated in Refs. 11 and 36. The values of K_{Ic} calculated for the initial and subsequent propagations in TSE-5, -5A, and -6, are given in Ref. 37. The values of K_{Ic} for TSE-7 are given in Ref. 38. Table 4 lists the values of K_{Ic} calculated for all the initiation events in TSE-5, -5A, -6 and -7. The initial flaws in TSE-5, -5A, and -6 were long, two-dimensional surface flaws. The initial flaw in TSE-7

was a short, finite-length, three-dimensional surface flaw. The method of calculating the values of K_{Ic} for the two-dimensional flaws in the TSEs is discussed in Ref. 39. The post-test three-dimensional analysis of the initial flaw in TSE-7 is discussed in Ref. 38. The values of K_{Jc} measured with small characterization specimens taken, before the tests, from the prolongations of the test cylinders, and afterwards, from the test cylinders themselves, are given in Refs. 38 and 40. For the analyses to be discussed here, only the characterization data obtained from specimens taken from the test cylinders themselves, or specimens taken from the matching prolongations and given the same heat treatment that was applied to the test cylinders, are considered. The characterization data are listed in Appendix B. The values of T_o calculated from the toughness characterization data for the materials of the TSE cylinders are given in Table 4. For these calculations of T_o, it was assumed, based on a previous study,[41] that the transition temperature range ends at the temperature of onset of the Charpy upper shelf, and these temperatures, designated T_{US}, are also listed in Table 4.

The results summarized in Table 4 are plotted in Fig. 9, which demonstrates clearly that the values of K_{Ic} calculated for the ORNL TSEs are well estimated by the proposed Weibull E399 procedure. In the case of these data, because of the variability of the individual yield stress values with both material and test temperature, Eq. (19) was used to produce a single value of σ_R = 153 MPa, calculated from 483 MPa /$\sqrt{10}$, with no apparent loss of accuracy. Figure 9 also demonstrates an additionally important fact, namely that the fracture toughness for the initial flaw in TSE-7, which was a short, finite-length surface flaw, shows no apparent elevation with respect to the toughness values governing the extension of the other much longer initial flaws.

Recent experiments and analytical investigations at ORNL[42] have focused on defining the effects of shallow crack depths and biaxial nominal stresses on fracture toughness. Experimental data obtained with uniaxially loaded beams and biaxially loaded cruciform beam specimens show that, once nominal yielding commences, specimens containing shallow cracks display increased toughness as the transverse nominal stress ratio decreases from unity toward zero. However, the previously obtained ORNL TSE data discussed here displayed no such effects, apparently both because the cylinders remained essentially elastic up to the point of fracture and because the transverse stress ratios at the

Table 3. Summary of test conditions for ORNL thermal shock experiments

Parameter	Experiment			
	TSE-5	TSE-5A	TSE-6	TSE-7
Test cylinder	TSC-1	TSC-2	TSE-3	TSC-4
Prolongation	TSP-1	TSP-2	TSP-3	TSP-4
Cylinder dimensions, as-tested, mm				
Outside diameter	991	991	991	991
Wall thickness	152	152	76	152
Length	1220	1220	1220	1220
Cylinder material	A508, class 2 chemistry			
Designation (A508 class 2)				
Tempering temperature, °C	613	679	613	704
RT_{NDT}, °C	66	10	66	-1
Yield stress at 22°C, MPa	682	581	682	449
Flaw (initial)				
Type[a]	LS	LS	LS	SCS
Orientation	axial	axial	axial	axial
Length, mm	1220	1220	1220	37
Depth, mm	16	11	7.6	14
Thermal shock				
Initial temperature of cyclinder,	96	96	96	96
°C	-196	-196	-196	-196
Initial temperature of coolant, °C	LN_2	LN_2	LN_2	LN_2
Quench medium[b]				

[a]LS = long, surface, SCS = semicircular, surface.
[b]LN_2 = liquid nitrogen.

Table 4. Characterization data and K_{Ic} values for ORNL thermal shock experiments TSE-5, -5A, -6, and 7

TSE	T_{US} (°C)	T (°C)	T_o (°C)	$T - T_o$ (°C)	K_{Ic} (MPa$\sqrt{m}$)
5	110	-9	-15	6	79
		-3		12	11
		79		94	115
5A	40	-11	-44	33	70
		12		56	85
		13		57	108
		21		65	135
6	110	-12	-23	11	46
		-28		-5	87
7	80	-19	-31	12	55[a]
		8		39	108
		31		62	117

[a]Three dimensional.

inside surface for thermal loading were, in accordance with theory,[43] always unity. Despite the importance of these results, they have not always been given the full weight they deserve in the body of evidence concerning shallow-crack and biaxial-stress effects, partly because of a degree of uncertainty concerning the possible effects of residual stresses on the initial values of K_{Ic} calculated for the TSEs. For this reason, analyses have recently been developed to estimate the residual stress patterns in the TSE cylinders, as tested, based on the surface measurements of residual strains in the cylinders made before and after final machining, and graphical estimates of the through-thickness residual stress distributions existing before final machining.[13] From these estimates of residual stresses, adjustments to the K_{Ic} values calculated for the initial flaws in the TSEs have been determined.[13] In all cases, the adjustments, which are listed in Table 5, are small and they do not change the conclusions drawn from the TSE data without considering residual stresses. The values of K_{Ic} for the initial flaws in the TSEs, adjusted for the effects of residual stresses, are shown by the triangles in Fig. 9, along with the values calculated prior to adjustment, indicated by the circles.

Table 5. Adjustments to K_{Ic} values for initial flaws in ORNL thermal shock experiments for effects of residual stresses

TSE	Flaw dimensions (mm)		Surface residual stress (MPa)	$K_{I(res)}$ (MPa$\sqrt{m}$)
	Depth	Length		
5	16	1220	-120	-7.27
5A	11	1220	-70	-5.54
6	7.6	1220	1.5	0.26
7	14	37	-70	-5.52

DISCUSSION

The results presented here bear directly on the question of whether, for engineering purposes, the concept of K_{Ic} is valid for ferritic steels. Pragmatically, the evidence presented supports the premise that size effects, due both to statistics and constraint variations, do exist, but that these size effects become small enough as crack length increases to be treated as effectively vanishing at predictable crack lengths, thus preserving the concept of K_{Ic}. Additionally, due possibly to the equibiaxiality of surface thermal stresses in cylinders, no toughness elevation for short, finite-length, surface cracks was evident in the ORNL TSE data with respect to the toughnesses governing the extensions of much longer cracks. Furthermore, no toughness elevations with respect to K_{Ic} were observed in the ORNL TSE data due to shallow crack depth or biaxiality of nominal stress. Since the ORNL thermal shock experiments produced applied K_{Ic} values in the same range as those hypothetically expected to occur due to PTS loading in the RPVs,[13] the results here are directly relevant to the integrity analysis of RPVs.

Potential applications of the approach described here are numerous, including any fracture control plan for a ferritic structural or pressure vessel steel for which small fracture-mechanics specimens can be made and tested, or the characterizing temperature

T_o reliably estimated by other means. Important examples include RPVs subjected to irradiation and containing relatively small surveillance specimens; tanks, pipes and pipelines subjected to internal pressure, especially if also exposed to low temperatures; and structures containing non-stress-relieved welds, stress concentrations, and/or

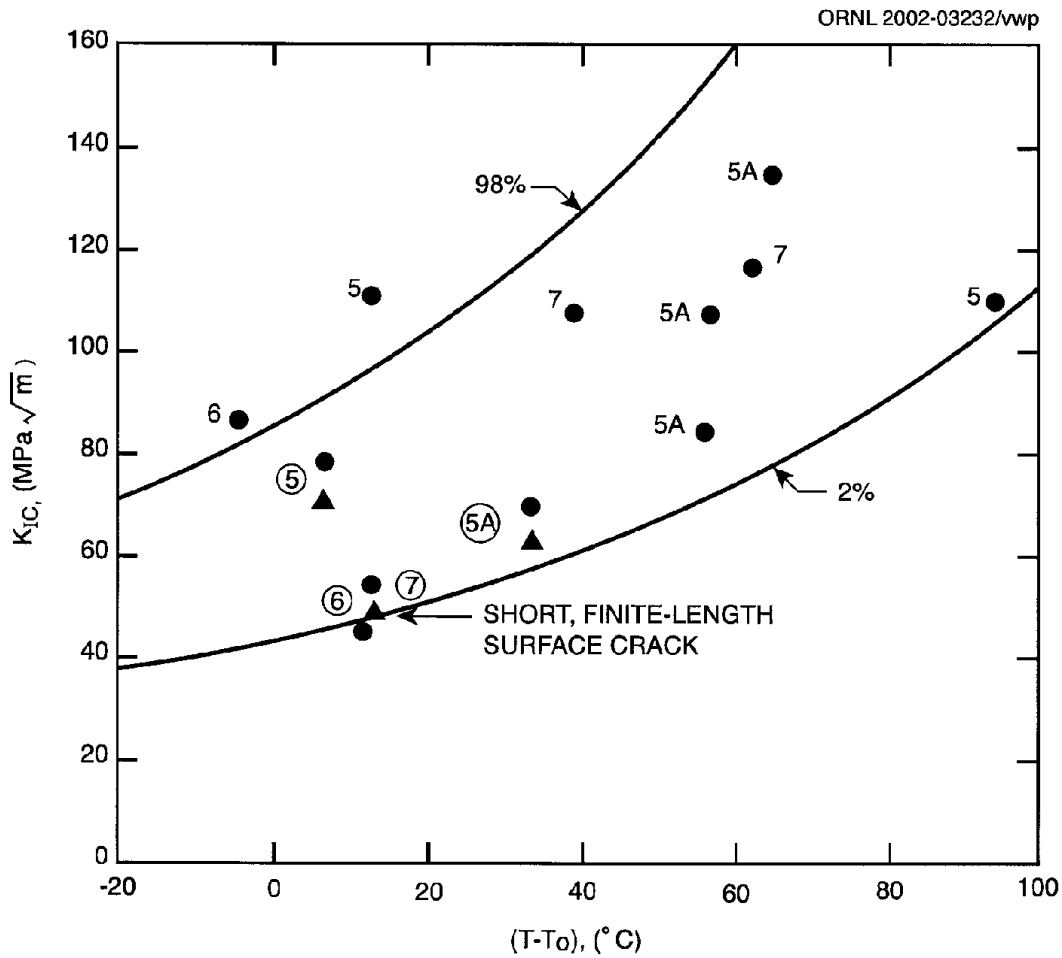

Figure 9. Plot of K_{Ic} values calculated directly from ORNL thermal shock data, where corresponding T_o values are calculated from small specimen K_{Jc} data and tolerance bound curves are based on σ_R = 153 MPa; values of K_{Ic} for initial flaws, indicated by circled numbers, are plotted without (as filled circles) and with (as filled triangles) minor adjustments for the effects of residual stress.

connections subject to multiaxial stress. In the case of irradiated reactor pressure vessels, multiple methods of determining T_o are under investigation. Some of these methods are direct,[3,25,32] and some are indirect,[44] but regardless of the exact procedure to be applied in a given case, the opportunity to base statistical calculations of valid K_{Ic} values, directly or indirectly, on small-specimen fracture toughness data presents a distinct advantage.

CONCLUSIONS

A statistical description of valid K_{Ic} data for the ferritic steels typically used in structures, piping, and pressure vessels has been derived by combining the principles of the elastic-plastic Master Curve of ASTM E 1921 and the criterion for validity under elastic conditions contained in ASTM E 399. By all appearances, the results agree well with the ASME K_{Ic} database, considering only its LEFM valid data, as well as HSST Plate 02 and the ORNL thermal shock data, calculations for the latter two cases having produced estimates of K_{Ic}, based on small specimen K_{Jc} data, that agree well with the available, directly measured, values of K_{Ic}. Thus, the proposed method appears to offer a promising approach for estimating values of K_{Ic} and their statistics based on small-specimen fracture toughness data.

ACKNOWLEDGMENTS

The authors express their appreciation to the U.S. Nuclear Regulatory Commission for the sponsorship of this research task under the Heavy-Section Steel Irradiation (HSSI) Program and to Julia L. Bishop for the preparation of the manuscript.

REFERENCES

1. ASTM Standard E 1921-97, "Test Method for Determination of Reference Temperature, $T_{o,}$ for Ferritic Steels in the Transition Range," *Annual Book of ASTM Standards*, Vol. 03.01, American Society for Testing and Materials, West Conshohocken, Pa., 2001.

2. *ASME Boiler and Pressure Vessel Code*: *An American National Standard*, Appendix A, "Analysis of Flaws," Section XI, Rules for Inservice Inspection of Nuclear Power Plant Components, American Society of Mechanical Engineers, New York, 1998.

3. J. G. Merkle, K. Wallin, and D. E. McCabe, *Technical Basis for an ASTM Standard on Determining the Reference Temperature, T_o, for Ferritic Steels in the Transition Range*, NUREG/CR-5504 (ORNL/TM-13631), November 1998.

4. D. E. McCabe, J. G. Merkle, and K. Wallin, "Technical Basis for the Master Curve Concept of Fracture Toughness Evaluations in the Transition Range," pp. 21-33 in *Fatigue and Fracture Mechanics: 30th Volume, ASTM STP 1360*, P. C. Paris and K. L. Jerina, Eds., American Society for Testing and Materials, West Conshohocken, Pa., 2000.

5. M. A. Sokolov, "Statistical Analysis of the ASME K_{Ic} Database," *Journal of Pressure Vessel Technology*, *Transactions of the ASME*, Vol. 120, February 1998, pp. 24-28.

6. W. A. Van der Sluys et al., "Fracture Toughness Master Curve Development: Fracture Toughness of Ferritic Steels, Reference Temperature T_o," *WRC Bulletin 457*, Welding Research Council, Inc., New York, December 2000.

7. W. A. Van der Sluys et al., "Fracture Toughness Master Curve Development: Application of Master Curve Fracture Toughness Methodology for Ferritic Steels," *WRC Bulletin 458*, Welding Research Council, Inc., New York, January 2001.

8. W. A. Van der Sluys et al., "Fracture Toughness Master Curve Development: Strategies for RPV Assessment," *WRC Bulletin 459*, Welding Research Council, Inc., New York, February 2001.

9. K. K. Yoon, "Summary of Technical Basis for Direct Application of Master Curve in Section XI of ASME Code: Code Case N-XXX," Attachment 16 to Minutes of the ASME Section XI Working Group on Flaw Evaluation, February 13, 2001.

10. D. E. McCabe, J. G. Merkle, and R. K. Nanstad, "A Perspective on Transition Temperature and K_{Jc} Data Characterization," pp. 215-232 in *Fracture Mechanics: Twenty-Fourth Volume, ASTM STP 1207*, J. D. Landes, D. E. McCabe, and J. A. M. Boulet, Eds., American Society for Testing and Materials, Philadelphia, 1994.

11. R. D. Cheverton, S. K. Iskander, and D. G. Ball, "Review of Pressurized-Water Reactor-Related Thermal Shock Studies," pp. 752-766 in *Fracture Mechanics: Nineteenth Symposium, ASTM STP 969*, American Society for Testing and Materials, Philadelphia, 1988.

12. J. G. Merkle, "Patterns and Perspectives in Applied Fracture Mechanics," pp. 3-40 in *Fracture Mechanics: 26th Volume, ASTM STP 1256*, W. G. Reuter, J. H. Underwood, and J. C. Newman, Eds., American Society for Testing and Materials, Philadelphia, 1995.

13. J. G. Merkle, *Estimates of Residual Stress Effects on Fracture Toughness Values Calculated for Thermal Shock Tests Performed at ORNL*, ORNL/NRC/LTR-99/31, Oak Ridge National Laboratory, Oak Ridge, Tenn., April 2000.

14. F. A. McClintock, "Slip Line Fracture Mechanics: A New Regime of Fracture Mechanics," in *Fatigue and Fracture Mechanics: 33rd Volume, ASTM STP 1417*, W. G. Reuter and R. S. Piascik, Eds., American Society for Testing and Materials, West Conshohocken, Pa., to be published in 2002.

15. K. Wallin, "Statistical Modelling of Fracture in the Ductile-to-Brittle Transition Region," pp. 415-445 in *Defect Assessment in Components - Fundamentals and Applications*, ESIS/EGF9, J. G. Blauel and K.-H. Schwalbe, Eds., Mechanical Engineering Publications, London, 1991.

16. T. U. Marston, Ed., *Flaw Evaluation Procedures: Background and Application of ASME Section XI, Appendix A*, EPRI NP-719-SR, prepared by the ASME Section XI Task Group on Flaw Evaluation, Electric Power Research Institute, Palo Alto, Calif., August 1978, with Errata dated April 14, 1980.

17. R. K. Nanstad, J. A. Keeney, and D. E. McCabe, *Preliminary Review of the Bases for the K_{Ic} Curve in the ASME Code*, ORNL/NRC/LTR-93/15, Oak Ridge National Laboratory, Oak Ridge, Tenn., July 1993.

18. K. Wallin, "Statistical Re-Evaluation of the ASME K_{Ic} and K_{IR} Fracture Toughness Reference Curves," *Nuclear Engineering and Design*, 193, 317-326 (1999).

19. K. O. Bowman and P. T. Williams, *Technical Basis for Statistical Models of Extended K_{Ic} and K_{Ia} Fracture Toughness Databases for RPV Steels*, ORNL/NRC/LTR-99/27, Oak Ridge National Laboratory, Oak Ridge, Tenn., February 2000.

20. P. T. Williams, K. O. Bowman, B. R. Bass, and T. L. Dickson, "Weibull Statistical Models of K_{Ic} and K_{Ia} Fracture Toughness Databases for Pressure Vessel Steels with an Application to Pressurized Thermal Shock Assessments of Nuclear Reactor Pressure Vessels," presented at IAEA Specialists' Meeting on Methodology and Supporting Research for the Pressurized Thermal Shock Evaluation, Rockville, Md., July 18-20, 2000.

21. M. T. Kirk, *Recommended Method to Account for Uncertainty in the Fracture Toughness Characterization Used to Re-Evaluate the Pressurized Thermal Shock (PTS) Screening Criteria*, draft NUREG report, U.S. Nuclear Regulatory Commission, Washington, D.C., August 31, 2001.

22. D. E. McCabe and J. G. Merkle, "Estimation of Lower-Bound K_{Jc} on Pressure Vessel Steels from Invalid Data," pp. 198-213 in *Fatigue and Fracture Mechanics: 28th Volume, ASTM STP 1321*, J. H. Underwood, B. D. MacDonald, and M. R. Mitchell, Eds., American Society for Testing and Materials, West Conshohocken, Pa., 1997.

23. *ASME Boiler and Pressure Vessel Code: An American National Standard*, Code Case N-629, "Use of Fracture Toughness Test Data to Establish Reference Temperature for Pressure Retaining Materials," Section XI, Division 1, American Society of Mechanical Engineers, New York, May 7, 1999.

24. *ASME Boiler and Pressure Vessel Code: An American National Standard*, Code Case N-631, "Use of Fracture Toughness Test Data to Establish Reference Temperature for Pressure Retaining Materials Other than Bolting for Class 1 Vessels," Section III, Division 1, American Society of Mechanical Engineers, New York, September 24, 1999.

25. D. E. McCabe and M. A. Sokolov, "Experimental Validation Work to Prove the Master Curve Concept," presented at the COBEM-99 Conference, Aquas de Lindoia, Brazil, Nov. 22-26, 1999 (additional viewgraphs include Fig. 4). See also pp. 29-34 in *Fatigue and Weld Residual Stress*, PVP-Vol. 393, American Society of Mechanical Engineers, New York, 1999.

26. J. G. Merkle and R. K. Nanstad," Master Curve Derived Fracture Toughness and a Statistical Representation of Valid K_{Ic} Data," presented at Meeting on RT_{NDT} Uncertainty Characterization, U.S. Nuclear Regulatory Commission, Rockville, Md., December 19, 2000.

27. J. G. Merkle, *An Examination of the Size Effects and Data Scatter Observed in Small-Specimen Cleavage Fracture Toughness Testing*, NUREG/CR-3672 (ORNL/TM- 9088), Oak Ridge National Laboratory, Oak Ridge, Tenn., April 1984.

28. D. E. McCabe, *A Comparison of Weibull and β_{Ic} Analysis of Transition Range Fracture Toughness Data*, NUREG/CR-5788 (ORNL/TM-11959), Oak Ridge National Laboratory, Oak Ridge, Tenn., January 1992.

29. D. E. McCabe, "A Comparison of Weibull and β_{Ic} Analyses of Transition Range Data," pp.80-94 in *Fracture Mechanics: Twenty-Third Symposium, ASTM STP 1189*, American Society for Testing and Materials, West Conshohocken, Pa., 1993.

30. F. J. Loss, *Dynamic Tear Test Investigations of the Fracture Toughness of Thick-Section Steel*, NRL Report 7056 (HSSTP-TR-7), Naval Research Laboratory, Washington, D.C., May 14, 1970.

31. W. O. Shabbits, W. H. Pyle, and E. T. Wessel, *Heavy Section Fracture Toughness Properties of A533 Grade B Class I Steel Plate and Submerged-Arc Weldments*, WCAP-7414 (HSSTP-TR-6), Westinghouse Electric Corp., Pittsburgh, December 1969.

32. M. A. Sokolov, K. Wallin, and D. E. McCabe, "Application of Small Specimens to Fracture Mechanics Characterization of Irradiated Pressure Vessel Steels," pp. 263-279 in *Fatigue and Fracture Mechanics: 28th Volume*, ASTM STP 1321, J. H. Underwood, B. D. MacDonald, and M. R. Mitchell, Eds., American Society for Testing and Materials, West Conshohocken, Pa., 1997.

33. J. G. Merkle, "An Approximate Method of Elastic-Plastic Fracture Analysis for Nozzle Corner Cracks," pp. 674-702 in *Elastic-Plastic Fracture, ASTM STP 668*, J. D. Landes, J. A. Begley, and G. A. Clarke, Eds., American Society for Testing and Materials, Philadelphia, 1979.

34. K. Wallin, "Re-Evaluation of Thermal Shock Experiment Results Based on the VTT Approach for Statistical Treatment of Fracture Toughness Data," *Nuclear Engineering and Design*, 174, 205-218 (1997).

35. K. R. W. Wallin, "K_{Ic} - A Non-Measure of Plane Strain Fracture Toughness," Paper ICF10065OR, *Advances in Fracture Research*, Proceedings of the 10th International Congress on Fracture, Honolulu, December 2-6, 2001.

36. R. D. Cheverton and D. G. Ball, "The Role of Crack Arrest in the Evaluation of PWR Pressure Vessel Integrity During PTS Transients," *Engineering Fracture Mechanics*, 23(1), 710-80 (1986).

37. R. D. Cheverton et al., "Fracture Mechanics Data Deduced from Thermal-Shock and Related Experiments with LWR Pressure Vessel Material," *Journal of Pressure Vessel Technology*, 105, 102-110 (May 1983).

38. R. D. Cheverton et al., *Pressure Vessel Fracture Studies Pertaining to the PWR Thermal-Shock Issue: Experiment TSE-7*, NUREG/CR-4304 (ORNL/TM-6177), Oak Ridge National Laboratory, Oak Ridge, Tenn., August 1985.

39. S. K. Iskander, "A Method for LEFM Analysis of RPV During SBLOCA," *International Journal of Pressure Vessels and Piping*, 25, 279-298 (1986).

40. R. D. Cheverton et al., *Pressure Vessel Fracture Studies Pertaining to the PWR Thermal-Shock Issue: Experiments TSE-5, TSE-5A, and TSE-6*, NUREG/CR-4249 (ORNL/TM-6163), Oak Ridge National Laboratory, Oak Ridge, Tenn., June 1985.

41. J. G. Merkle, "Fracture Safety Analysis Concepts for Nuclear Pressure Vessels, Considering the Effects of Irradiation," *Journal of Basic Engineering*, Vol. 93, Series D, No. 2, 265-273 (June 1971).

42. B. R. Bass, P. T. Williams, W. J. McAfee, and C. E. Pugh, "Development of a Weibull Model of Cleavage Fracture Toughness for Shallow Flaws in Reactor Pressure Vessel Material," Paper No. ICONE9051, International Conference in Nuclear Engineering (ICONE9), Lyon, France, 2001.

43. S. P. Timoshenko and J. N. Goodier, *Theory of Elasticity*, Third Ed., McGraw-Hill, New York, 1987.

44. M. A. Sokolov and R. K. Nanstad, *Comparison of Irradiation-Induced Shifts of K_{Jc} and Charpy Impact Toughness for Reactor Pressure Vessel Steels*, NUREG/CR-6609, Oak Ridge National Laboratory, Oak Ridge, Tenn., November 2000.

APPENDIX A
EQUATIONS FOR CUMULATIVE PROBABILITY AND PROBABILITY DENSITY FUNCTIONS FOR K_{Ic}

For a given value of $(T - T_o)$, the relation between the cumulative probability, P_f, and K_{Ic} is determined in two steps. The first step is to combine Eqs. (3) and (4) and rearrange to obtain

$$K_{Jc(1T)} = K_{\min} \left\{ 1 + \frac{\left[\left(\frac{K_{Ic}}{K_{\min}} \right)^{3/2} - \left(\frac{K_{Ic}}{K_{\min}} \right)^{1/2} \right]}{\left(\frac{\sqrt{B_1/\alpha_o}}{K_{\min}/\sigma_Y} \right)^{1/2}} \right\}, \tag{A.1}$$

in which B_1 is set equal to the thickness of a 1T specimen. Then, after obtaining the value of $(K_o - K_{min})$ from Eq. (12), that value and the value of $K_{Jc(1T)}$ obtained from Eq. (A.1) are entered into Eq. (9) to obtain P_f.. For values of K_{Ic} equal to or less than the value determined from Eq. (17), $K_{Ic} = K_{Jc(1T)}$ and P_f is determined by Eqs. (9) and (12) without the use of Eq. (A.1). Equations (9), (12), and (A.1) also facilitate calculations of the values of P_f for points along the repositioned ASME K_{Ic} curve defined by Eq. (16) and plotted in Fig. 4. These values range between 7% near $(T - T_o) = 40°C$, to slightly above 1% near $(T - T_o) = -30°C$, with a minimum of 1% near $T = T_o$. These results agree well with the graphical estimates in Fig. 4.

Calculations of the pdf for K_{Ic} can be made conveniently in closed form by employing the chain rule, according to which

$$pdf = \frac{dP_f}{dK_{Ic}} = \frac{dP_f}{dK_{Jc(1T)}} \cdot \left[\frac{1}{K_{\min}} \cdot \frac{dK_{Jc(1T)}}{d\left(\frac{K_{Ic}}{K_{\min}} \right)} \right]. \tag{A.2}$$

The first factor in Eq. (A.2) is obtained by differentiation of Eq. (9), giving

$$\frac{dP_f}{dK_{Jc(1T)}} = \frac{4(K_{Jc(1T)} - K_{\min})^3}{(K_o - K_{\min})^4} \; e^{-\left(\frac{K_{Jc(1T)} - K_{\min}}{K_o - K_{\min}}\right)^4}, \tag{A.3}$$

in which (K_o - K_{min}) is obtained from Eq. (12) and ($K_{Jc(1T)}$ - K_{min}) is obtained from Eq. (A.1). The second factor in Eq. (A-2) is obtained by differentiating Eq. (A.1) to give

$$\frac{1}{K_{\min}} \cdot \frac{dK_{Jc(1T)}}{d\left(\frac{K_{Ic}}{K_{\min}}\right)} = \frac{\frac{3}{2}\left(\frac{K_{Ic}}{K_{\min}}\right)^{1/2} - \frac{1}{2}\left(\frac{K_{Ic}}{K_{\min}}\right)^{-1/2}}{\left(\frac{\sqrt{B_1/\alpha_o}}{K_{\min}/\sigma_Y}\right)^{1/2}} . \tag{A.4}$$

For values of K_{Ic} equal to or less than the value determined from Eq. (17), $K_{Ic} = K_{Jc(1T)}$ and the pdf is determined from Eqs. (12) and (21) without the use of Eq. (A.4). Plots of the cumulative probability distributions for K_{Ic}, for (T - T_o) = -83.3, 0, and +44.4 °C (-150, 0, and +80°F), with σ_Y = 482.6 MPa (70 ksi) and α_o = 2.5, are shown in Fig. A.1. The value of σ_Y = 482.6 (70 ksi) is chosen as a representative value for the ASME K_{Ic} database, and the value of α_0 = 2.5 is chosen as the LEFM validity coefficient in ASTM E 399. The corresponding plots of the pdf are shown in Fig. A.2. The change of functions at the toughness at and below which $K_{Jc(1T)} = K_{Ic}$ causes slight oscillations in the pdf, most noticeably at low temperatures, but this has no effect on the mathematical relationship between the pdf, the cdf, and the tolerance bound functions.

In applying the standard three-parameter Weibull distribution represented by Eq. (9), it is recognized that the minimum toughness, K_{min}, is a mathematical fitting parameter rather than a parameter with precise physical significance.[3] The advantages of this approach are its simplicity and the resulting optimization of data-fitting for the majority of data. The potential disadvantage of assuming K_{min} = const. is that calculated probabilities of initiation may be overestimated at low applied values of K_I. However, most of the excess probabilities of initiation are likely to be offset by calculations of immediate crack arrest.

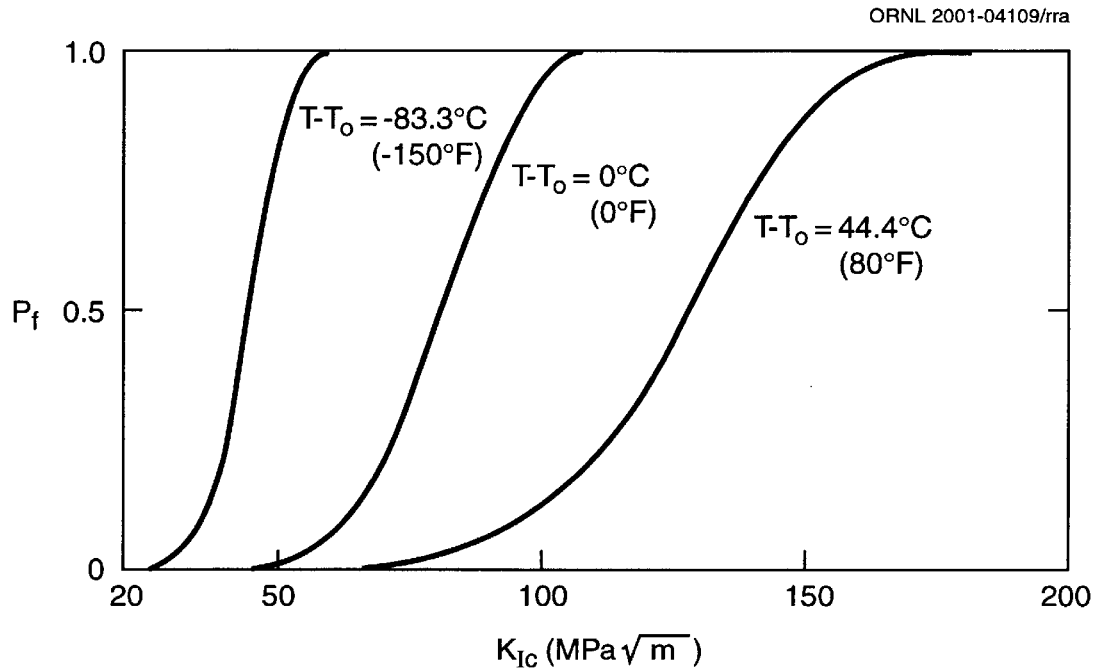

Figure A.1. Calculated cumulative probability curves for $(T - T_o) = -83.3$, 0, and 44.4°C, for $\sigma_Y = 482.6$ MPa (70 ksi) and $\alpha_o = 2.5$.

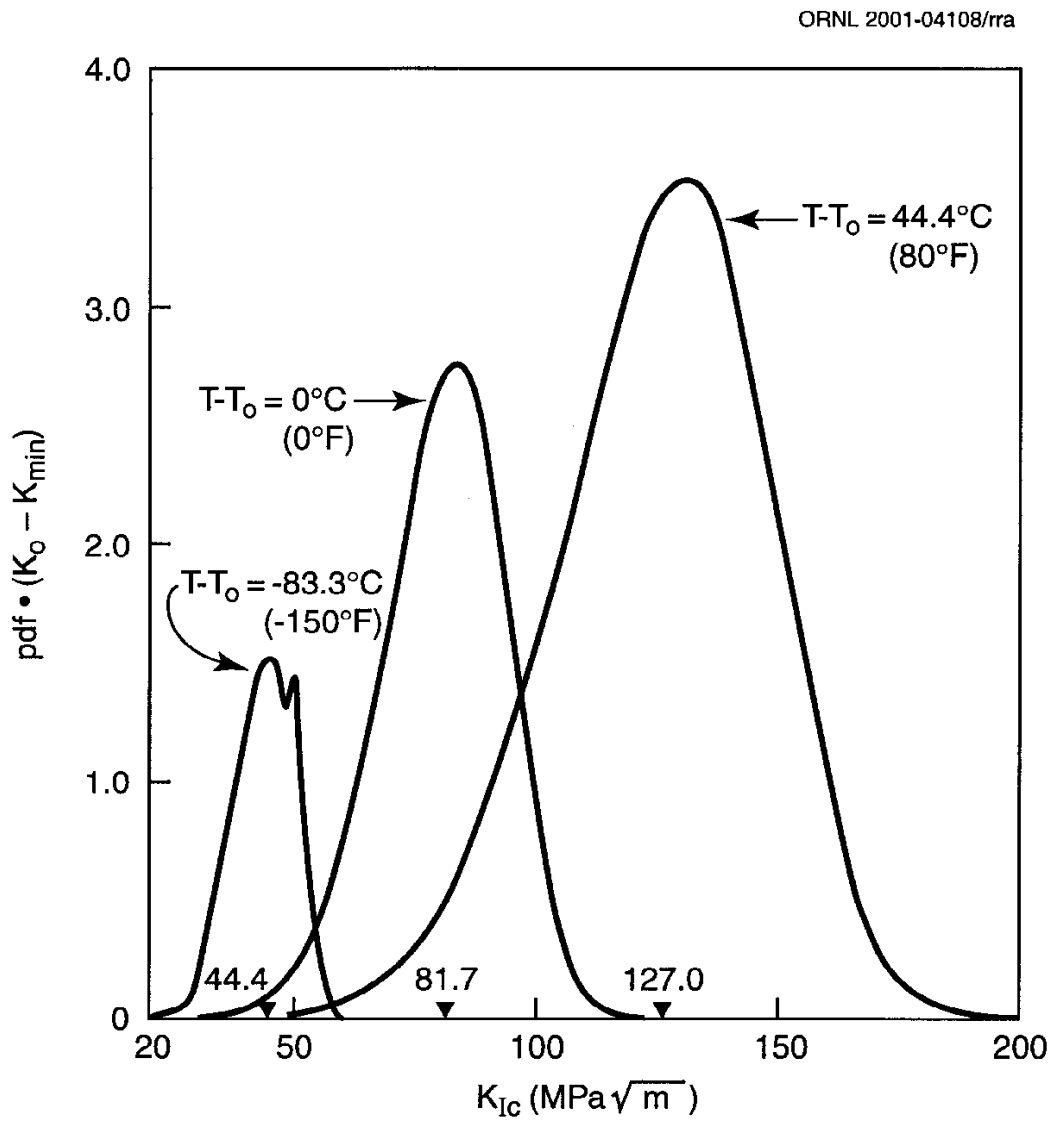

Figure A.2. Calculated probability density function curves, scaled by (K_o - K_{min}), for (T - T_o) = -83.3, 0, and 44.4°C, for σ_Y = 482.6 MPa (70 ksi) and α_o = 2.5.

APPENDIX B

SMALL SPECIMEN FRACTURE TOUGHNESS CHARACTERIZATION DATA FOR ORNL THERMAL SHOCK EXPERIMENTS

Test temperature, T (°C)	Yield stress, σ_Y (MPa)	Specimen thickness, B (mm)	Measured fracture toughness, K_{Jc} (MPa$\sqrt{m}$)
TSE-5 (TSP-1)			
-73	763	10	62
-73	763	10	74
-73	763	10	100
-46	741	10	41
-46	741	10	53
-46	741	10	101
-18	719	10	57
-18	719	10	57
-18	719	10	65
-18	719	10	71
-18	719	10	72
-18	719	10	86
-18	719	10	86
-18	719	10	88
-18	719	10	95
-18	719	10	101
-18	719	10	103
-18	719	10	106
-18	719	10	123
-18	719	10	124
-18	719	10	125
-18	719	10	133
-18	719	10	134
-18	719	10	135
-18	719	10	142
-18	719	10	150
-18	719	10	153
-18	719	10	159
-18	719	10	161
-18	719	10	165
-18	719	10	167
-18	719	10	176
-18	719	10	184
-18	719	10	188

Test temperature, T (°C)	Yield stress, σ_Y (MPa)	Specimen thickness, B (mm)	Measured fracture toughness, K_{Jc} (MPa$\sqrt{m}$)
-18	719	25.4	82
-18	719	25.4	102
-18	719	25.4	111
-18	719	25.4	145
-18	719	50.8	51
-18	719	50.8	80
-18	719	50.8	92
-18	719	50.8	105
-18	719	50.8	111
10	702	10	103
10	702	10	125
10	702	10	158
10	702	10	168
10	702	10	205
10	702	10	214
32	689	25.4	70
32	689	25.4	114
32	689	25.4	153
32	689	25.4	164
32	689	25.4	186
32	689	25.4	188
32	689	25.4	202
32	689	50.8	105
32	689	50.8	115
32	689	50.8	172
32	689	50.8	221
38	687	10	114
38	687	10	149
38	687	10	183
38	687	10	197
38	687	10	202
38	687	10	224
82	663	25.4	128
82	663	25.4	200
82	663	25.4	204
82	663	25.4	211
82	663	25.4	236
82	663	25.4	240
82	663	25.4	249

Test temperature, T (°C)	Yield stress, σ_Y (MPa)	Specimen thickness, B (mm)	Measured fracture toughness, K_{Jc} (MPa$\sqrt{m}$)
82	663	50.8	135
82	663	50.8	161
82	663	50.8	197
82	663	50.8	255
82	663	50.8	273
82	663	50.8	277
82	663	50.8	284
82	663	50.8	298
TSE-5A (TSP-2, TSC-2)			
-32	643	25.4	72
-32	643	25.4	74
-32	643	25.4	79
-32	643	25.4	91
-32	643	25.4	94
-32	643	25.4	99
-32	643	25.4	100
-32	643	25.4	106
-32	643	25.4	116
-32	643	25.4	119
-32	643	25.4	121
-32	643	25.4	121
-32	643	25.4	131
-32	643	25.4	135
-32	643	25.4	138
-32	643	25.4	160
-32	643	25.4	161
-32	643	25.4	163
-32	643	25.4	165
-32	643	25.4	182

Test temperature, T (°C)	Yield stress, σ_Y (MPa)	Specimen thickness, B (mm)	Measured fracture toughness, K_{Jc} (MPa$\sqrt{m}$)
-4	619	25.4	106
-4	619	25.4	112
-4	619	25.4	112
-4	619	25.4	140
-4	619	25.4	143
-4	619	25.4	149
-4	619	25.4	177
-4	619	25.4	180
-4	619	25.4	186
-4	619	25.4	200
-4	619	25.4	206
-4	619	25.4	210
-4	619	25.4	224
-4	619	25.4	229
-4	619	25.4	240
-4	619	25.4	240
-4	619	25.4	243
-4	619	25.4	245
-4	619	25.4	249
-4	619	25.4	261
-4	619	25.4	275

Test temperature, T (°C)	Yield stress, σ_Y (MPa)	Specimen thickness, B (mm)	Measured fracture toughness, K_{Jc} (MPa$\sqrt{m}$)
24	603	25.4	158
24	603	25.4	195
24	603	25.4	198
24	603	25.4	222
24	603	25.4	233
24	603	25.4	235
24	603	25.4	238
24	603	25.4	247
24	603	25.4	249
24	603	25.4	251
24	603	25.4	254
24	603	25.4	259
24	603	25.4	261
24	603	25.4	262
24	603	25.4	265
24	603	25.4	268
24	603	25.4	277
24	603	25.4	279
24	603	25.4	287
24	603	25.4	288
24	603	25.4	289
24	603	25.4	292
24	603	25.4	296
24	603	25.4	323
24	603	25.4	334
24	603	25.4	338
38	599	25.4	220
38	599	25.4	260
38	599	25.4	275
38	599	25.4	276
38	599	25.4	277
38	599	25.4	281
TSE-6 (TSP-3, TSC-3)			
-73	763	25.4	38
-73	763	25.4	40
-73	763	25.4	42
-73	763	25.4	52
-73	763	25.4	52
-73	763	25.4	57
-73	763	25.4	59
-73	763	25.4	60
-73	763	25.4	61
-73	763	25.4	72

Test temperature, T (°C)	Yield stress, σ_Y (MPa)	Specimen thickness, B (mm)	Measured fracture toughness, K_{Jc} (MPa$\sqrt{m}$)
-46	741	25.4	46
-46	741	25.4	54
-46	741	25.4	57
-46	741	25.4	64
-46	741	25.4	70
-46	741	25.4	72
-46	741	25.4	81
-46	741	25.4	93
-46	741	25.4	100
-46	741	25.4	120
-32	731	25.4	49
-32	731	25.4	80
-32	731	25.4	87
-32	731	25.4	95
-32	731	25.4	97
-32	731	25.4	99
-32	731	25.4	104
-32	731	25.4	138
-32	731	25.4	144
10	702	25.4	72
10	702	25.4	87
10	702	25.4	110
10	702	25.4	113
10	702	25.4	125
10	702	25.4	128
10	702	25.4	129
10	702	25.4	135
10	702	25.4	135
10	702	25.4	169
10	702	25.4	175
10	702	25.4	177
10	702	25.4	197
10	702	25.4	200
10	702	25.4	201
66	672	25.4	164
66	672	25.4	233
66	672	25.4	247
66	672	25.4	249
66	672	25.4	263
66	672	25.4	264
66	672	25.4	265
66	672	25.4	270
66	672	25.4	275

Test temperature, T (°C)	Yield stress, σ_Y (MPa)	Specimen thickness, B (mm)	Measured fracture toughness, K_{Jc} (MPa$\sqrt{m}$)
TSE-7 (TSP-4)			
-101	550	25.4	37
-101	550	25.4	37
-101	550	25.4	38
-101	550	25.4	41
-101	550	25.4	43
-101	550	25.4	50
-101	550	25.4	50
-101	550	25.4	56
-46	490	25.4	59
-46	490	25.4	62
-46	490	25.4	67
-46	490	25.4	71
-46	490	25.4	73
-46	490	25.4	75
-46	490	25.4	75
-46	490	25.4	78
-46	490	25.4	101
-46	490	25.4	102
-18	465	25.4	95
-18	465	25.4	96
-18	465	25.4	105
-18	465	25.4	106
-18	465	25.4	125
-18	465	25.4	144
-18	465	25.4	162
-18	465	25.4	164
-18	465	25.4	197
-18	465	25.4	201
21	449	25.4	147
21	449	25.4	156
21	449	25.4	179
21	449	25.4	199
21	449	25.4	230
21	449	25.4	241
21	449	25.4	246
21	449	25.4	268
21	449	25.4	295
21	449	25.4	321

Test temperature, T (°C)	Yield stress, σ_Y (MPa)	Specimen thickness, B (mm)	Measured fracture toughness, K_{Jc} (MPa$\sqrt{m}$)
52	439	25.4	153
52	439	25.4	160
52	439	25.4	207
52	439	25.4	209
52	439	25.4	225
52	439	25.4	235
52	439	25.4	245
52	439	25.4	261
52	439	25.4	270
52	439	25.4	310

EXTERNAL DISTRIBUTION

1. N. C. Chokshi, RES/DET/MEB, U.S. Nuclear Regulatory Commission, Washington, DC 20555-0001
2. C. J. Fairbanks, RES/DET/MEB, U.S. Nuclear Regulatory Commission, Washington, DC 20555-0001
3. E. M. Hackett, RES/DET/MEB, U.S. Nuclear Regulatory Commission, Washington, DC 20555-0001
4. R. E. Hardies, RES/DET/MEB, U.S. Nuclear Regulatory Commission, Washington, DC 20555-0001
5. M. T. Kirk, RES/DET/MEB, U.S. Nuclear Regulatory Commission, Washington, DC 20555-0001
6. S.N.M. Malik, RES/DET/MEB, U.S. Nuclear Regulatory Commission, Washington, DC 20555-0001
7. M. E. Mayfield, Director, RES/DET, U.S. Nuclear Regulatory Commission, Washington, DC 20555-0001
8. M. A. Mitchell, NRR, U.S. Nuclear Regulatory Commission, MS-07-D4, Washington, DC 20555-0001
9. C. G. Santos, NMSS/SFPO, U.S. Nuclear Regulatory Commission, Washington, DC 20555-0001
10. R. L. Tregoning, RES/DET/MEB, U.S. Nuclear Regulatory Commission, Washington, DC 20555-0001
11. K. R. Wichman, NRR, U.S. Nuclear Regulatory Commission, MS-07-D4, Washington, DC 20555-0001
12. T. L. Anderson, Structural Reliability Technology, 2802 Sundown Lane, Suite 302, Boulder, CO 80303
13. W. H. Bamford, Westinghouse R&D Center, P.O. Box 2728, Pittsburgh, PA 15230-2728
14. W. Belcher, Engineering Division, British Energy, Ltd., Location 94, Barnwood, Gloucester, GL4 3RS, United Kingdom
15. J. M. Bloom, McDermott Technology, Inc., 1562 Beeson Street, Alliance, OH 44601
16. R. D. Cheverton, 2703 West Gallaher Ferry Road, Knoxville, TN 37932
17. R. C. Cipolla, APTECH Engineering Services, Inc., 1282 Reamwood Ave., Sunnyvale, CA 94089
18. R. H. Dodds, University of Illinois, 3140 Newmark Laboratory, 205 N. Matthews, Urbana, IL 61801
19. E. Eason, Modeling and Computing Services, Suite B, 6560 Gunpark Drive, Boulder, CO 80301
20. T. J. Griesbach, ATI Consulting, 2010 Crow Canyon Place, Suite 140, San Ramon, CA 94583
21. S. Hatano, Tokyo Research and Development Center (JAPEIC), Business Court, Shin-Urayasu, 1-9-2 Mihama Urayasushi, Chiba, Japan 2790011

22. J. A. Joyce, U.S. Naval Academy, Mechanical Engineering Dept. MS-11C, 590 Holloway Road, Annapolis, MD 21402
23. T. Kress, 102-B Newridge Road, Oak Ridge, TN 37830
24. J. D. Landes, University of Tennessee, 314 Perkins Hall, Knoxville, TN 37996-2030
25. D. P. G. Lidbury, Serco Assurance, Walton House, 404 The Quadrant, Risley, Warrington, Cheshire, WA3 6AT, United Kingdom
26. R. E. Link, U.S. Naval Academy, Mechanical Engineering Dept. MS-11C, 590 Holloway Road, Annapolis, MD 21402
27. R. G. Lott, Westinghouse, 1310 Beulah Rd., Pittsburgh, PA 15325
28. G. E. Lucas, College of Engineering, Department of Chemical Engineering, University of California, Ward Memorial Drive, Santa Barbara, CA 93106
29. E. Lucon, Reactor Materials Research, SCK-CEN, Boretang 200, B-2400, Mol, Belgium
30. T. R. Mager, Materials Reliability, Science and Technology Dept., Westinghouse Electric, 1332 Beulah Road, Pittsburgh, PA 15235

31-34. D. E. McCabe, 124 Newport Drive, Oak Ridge, TN 37830

35. G. R. Odette, College of Engineering, Department of Chemical Engineering, University of California, Ward Memorial Drive, Santa Barbara, CA 93106
36. S. D. Papka, Exxon-Mobil, Upstream Research Co., P.O. Box 2189, Houston, TX 77252-2189
37. R. H. Priest, Engineering Division, British Energy, Ltd., Location 94, Barnwood, Gloucester, GL4 3RS, United Kingdom
38. S. T. Rolfe, The University of Kansas, Lawrence, KS 66045-2235
39. S. T. Rosinski, EPRI, 1300 W. Wt. Harris Blvd., Charlotte, NC 28262-8550
40. D. A. Scarth, Ontario Hydro Research Division, 800 Kipling Ave., Toronto, Ontario, Canada M8Z 5S4
41. M. Serrano, CIEMAT, Nuclear Fission Dept., Auda. Complutense 22-28040, Madrid, Spain
42. W. L. Server, ATI Consulting, 24 Grenbarr Ct., Pinehurst, NC 28374
43. W. J. Shack, 837 Clyde Drive, Downers Grove, IL 60516
44. D. K. Shum, Saint-Gobain, Northboro R&D Center, Goddard Road, Northboro, MA 01532-1545
45. F. A. Simonen, Pacific Northwest Laboratories, P.O. Box 999, Richland, WA 99252
46. P. P. Smith, Exxon-Mobil, Upstream Research Co., P.O. Box 2189, Houston, TX 77252-2189
47. W. A. Van der Sluys, 1488 Glendking Lane, Alliance, OH 44601
48. E. Van Walle, Reactor Materials Research, SCK-CEN, Boretang 200, B-2400, Mol, Belgium
49. K. Wallin, VTT Manufacturing Technology, P.O. Box 1704, Kemistintie 3, Espoo, FIN-02044 VTT, Finland
50. T. J. Williams, Rolls-Royce, P.O. Box 2000, Raynesway, Derby, DE21 7XX, United Kingdom

51. K. K. Yoon, Framatome Technologies, 3315 Old Forest Road, P.O. Box 10935, Lynchburg, VA 24506-0935
52. S. Yukawa, 4925 Valkyrie Dr., Boulder, CO 80301

INTERNAL DISTRIBUTION

53. B. R. Bass
54. E. E. Bloom
55. W. R. Corwin
56. T. L. Dickson
57. R. G. Gilliland
58. L. L. Horton
59-62. J. G. Merkle
63. G. E. Michaels
64. D. L. Moses
65-68. R. K. Nanstad
69. J. B. Roberto
70-77. T. M. Rosseel
78. J. J. Simpson
79-82. M. A. Sokolov
83. R. E. Stoller
84. J. A. Wang
85. P. T. Williams
86. S. J. Zinkle